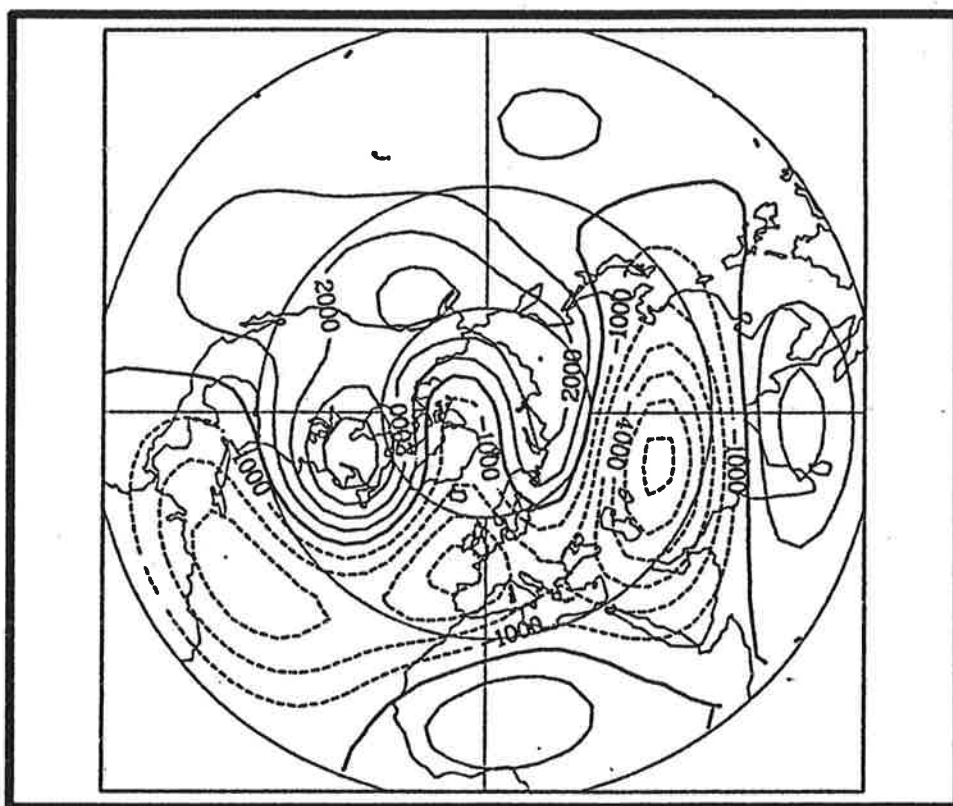




Max-Planck-Institut für Meteorologie

REPORT No. 41



NORTHERN HEMISPHERE ATMOSPHERIC RESPONSE TO CHANGES OF ATLANTIC OCEAN SST ON DECADAL TIME SCALES: A GCM EXPERIMENT

by

ANDREAS HENSE • RITA GLOWIENKA-HENSE
HANS VON STORCH • URSULA STÄHLER

HAMBURG, NOVEMBER 1989

AUTHORS:

ANDREAS HENSE

ALFRED WEGENER INSTITUT
FUER POLAR-UND MEERESFORSCHUNG
COLUMBUS CENTER
2850 BREMERHAVEN

RITA GLOWIENKA-HENSE

ALFRED WEGENER INSTITUT
FUER POLAR-UND MEERESFORSCHUNG
COLUMBUS-CENTER
2850 BREMERHAVEN

HANS VON STORCH

MAX-PLANCK-INSTITUT
FUER METEOROLOGIE

URSULA STAHLER

INSTITUT FUER GEOPHYSIK UND
METEOROLOGIE
UNIVERSITAET FRANKFURT
FELDBERGSTRASSE 47
6000 FRANKFURT

MAX-PLANCK-INSTITUT
FUER METEOROLOGIE
BUNDESSTRASSE 55
D-2000 HAMBURG 13
F.R. GERMANY

Tel.: (040) 4 11 73-0
Telex: 211092
Telemail: MPI.Meteorology
Telefax: (040) 4 11 73-298

**Northern Hemisphere atmospheric response to changes of
Atlantic Ocean SST on decadal time scales: a GCM experiment***

ANDREAS HENSE, RITA GLOWIENKA-HENSE

Alfred Wegener Institut für Polar- und Meeresforschung

HANS VON STORCH

MPI für Meteorologie Hamburg

URSULA STÄHLER

Institut für Geophysik und Meteorologie

Universität Frankfurt

*AWI-Publication No. 254
ISSN 0937-1060

ABSTRACT

Analyses indicate that the Atlantic Ocean SST was considerably colder at the beginning than in the middle of the century. Parallel to this a systematic change of the North Atlantic SLP pattern was observed. To find out whether the analyzed SST and SLP changes are consistent, which would indicate that the SST change was real and not an instrumental artifact, a response experiment with a low resolution (T21) atmospheric GCM was performed. Two perpetual January simulations were conducted which differ solely in Atlantic Ocean (40S - 60N) SST: the "cold" simulation utilizes the SSTs for the period 1904-13, the "warm" simulation uses the SST's for the period 1951-60. Also a "control" run, with the model's standard SST somewhat between the "cold" and "warm" SST, was made. For the response analysis a rigorous statistical approach was taken: First the null hypothesis of identical horizontal distributions was subjected to a multivariate significance test. Second, the level of recurrence was estimated. The multivariate statistical approaches are based on hierarchies of test models. We examined three different hierarchies: a scale dependent hierarchy based on spherical harmonics (S), and two physically motivated ones, one based on the barotropic normal modes of the mean 300 hPa flow (B) and one based on the eigenmodes of the advection diffusion operator at 1000 hPa (A).

The intercomparison of the "cold" and "warm" experiments indicates a signal in the geostrophic stream function that is in the S-hierarchy significantly nonzero and highly recurrent. In the A-hierarchy, the low level temperature field is identified as being significantly and recurrently affected by the altered SST distribution. The SLP signal is reasonably similar to the observed SLP change. Unexpectedly the upper level streamfunction signal does not appear significantly nonzero in the B-hierarchy. If, however the pairs of experiments "warm vs. control" and "cold vs. control" are examined in the B-hierarchy, a highly significant and recurrent signal emerges. We conclude that the "cold vs. warm" response is not a "small disturbance" which would allow the signal to be described by eigenmodes of the linearized system.

An analysis of the three-dimensional structure of the signal leads to the hypothesis that two different mechanisms are acting to modify the model's mean state. At low levels, the local heating and advection are dominant, but at upper levels the extratropical signal is a remote response to modifications of the tropical convection.

1. Introduction

1.1. DECADAL CHANGES OF NORTH ATLANTIC SST AND SLP

The time series of Atlantic Ocean sea surface temperatures (SST) show marked large scale low frequency variations on decadal time scales (Höfllich, 1974). This is exemplified by the dominant first two empirical orthogonal functions (EOFs) of SST in January (Fig. 1a,b) and their amplitudes from 1860 to 1960 (Fig. 1c,d). Both the patterns and the amplitudes for the other months are very similar to the January patterns and amplitudes. The pattern of the first EOF implies that its amplitude is related to an area average of the anomalous SST-field.

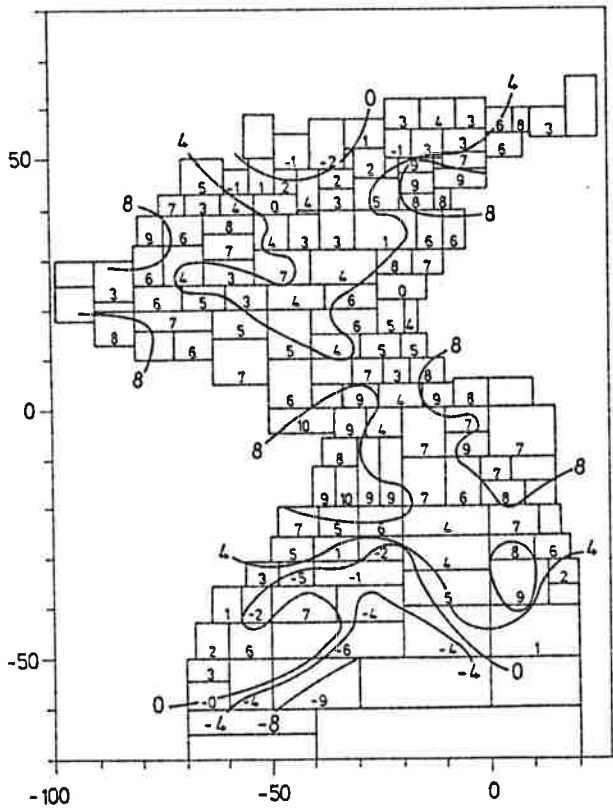
A period of anomalous low temperatures is observed from the beginning of the century until around 1920 while a period of positive temperature anomalies is found between 1950 and 1960. There is evidence that these changes are not an instrumental artifact but in part real: The HSST ("Historical Sea Surface Temperature"; Höfllich (1974)) data set is fairly homogeneous as it includes only bucket-reports. Also, similar temperature changes are reflected in air temperature records at Funchal on Madeira (Fig. 2). Furthermore Dickson et al.(1984) have shown that for the area west of Great Britain, the Atlantic was cooler by 1 - 2 °C and also fresher by 0.1 permille in the time around 1910 than in the time around the International Geophysical Year 1956.

Parallel to these oceanic changes there have also been observed changes in the atmosphere, in particular in the January sea level pressure (SLP) field over the North Atlantic. This is demonstrated in Fig. 3 which shows the (filtered, see below) decadal mean difference between surface pressure in the beginning and in the middle of the present century. This difference exhibits a large scale and coherent signal over the whole Atlantic - European sector (see discussion below).

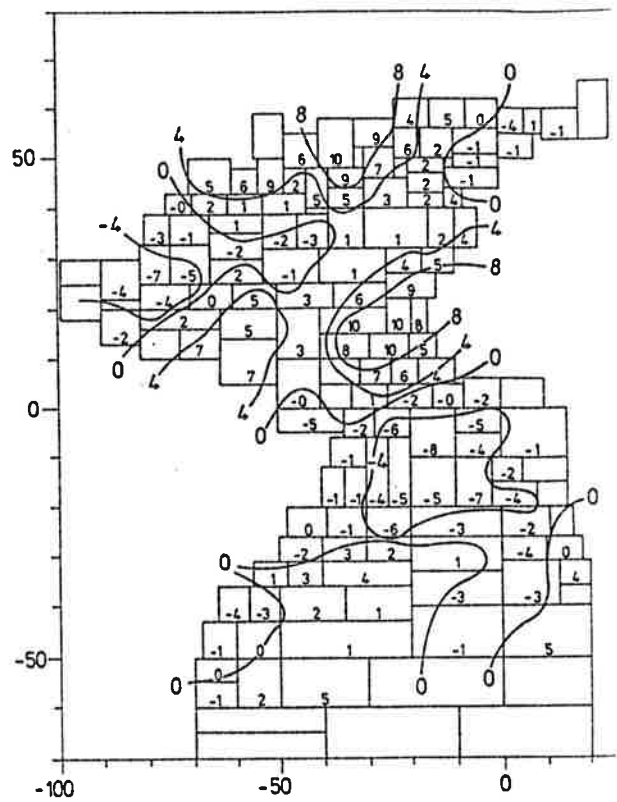
Questions to be asked are:

- * Are the changes real or artificial due to instrumental inhomogeneities and insufficient sampling?
- * Are the atmospheric changes a response to changed oceanic conditions or vice versa?

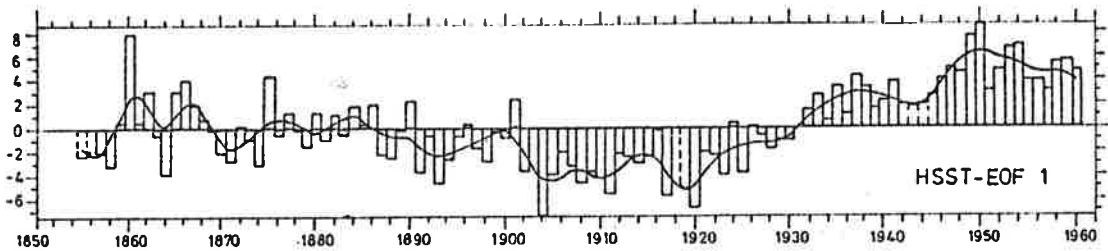
a) HSST-EOF 1 January 16.2%



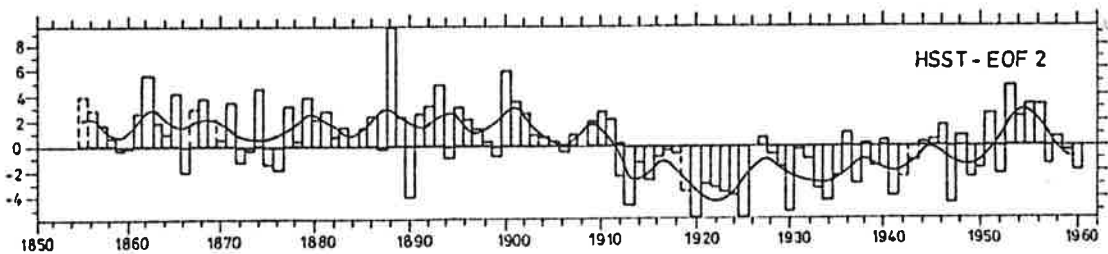
b) HSST-EOF 2 January 8.8%



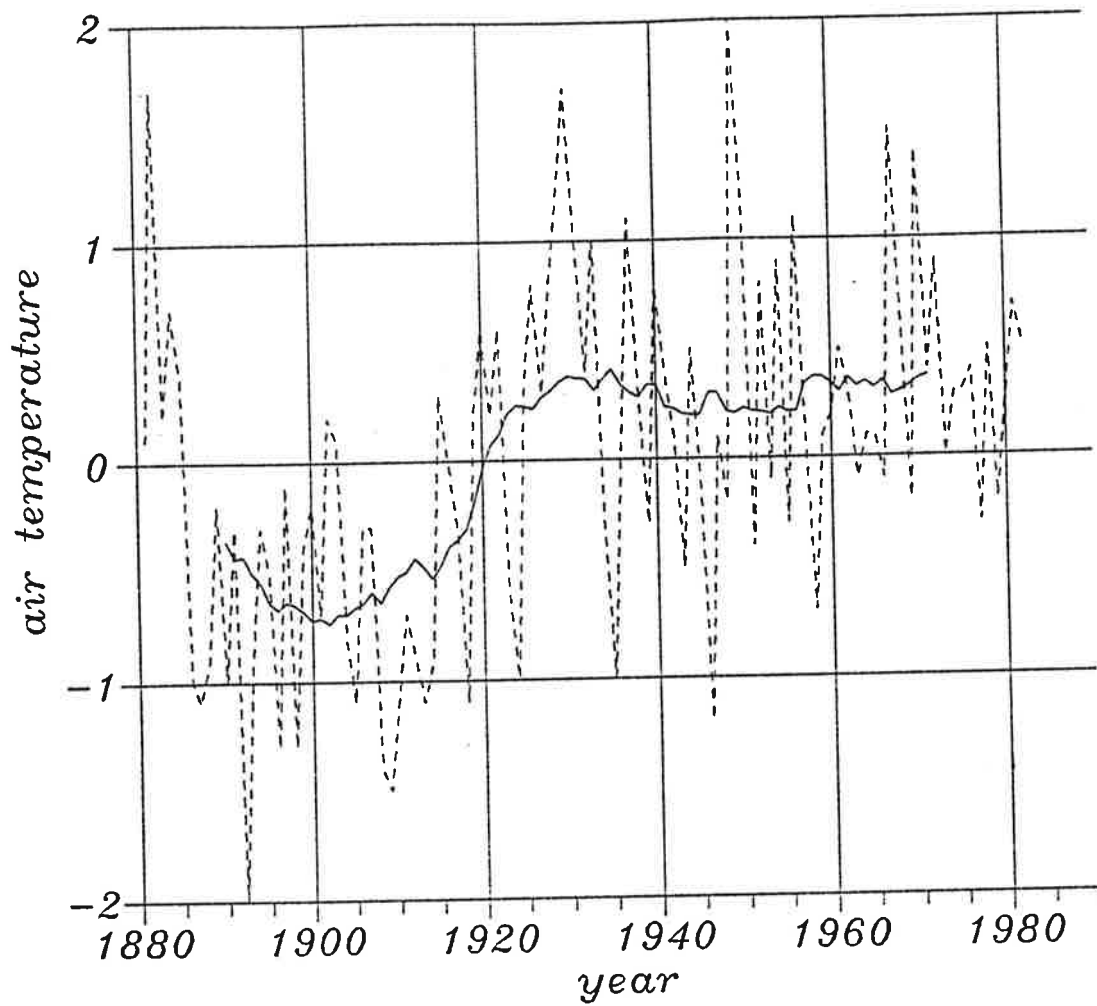
c)



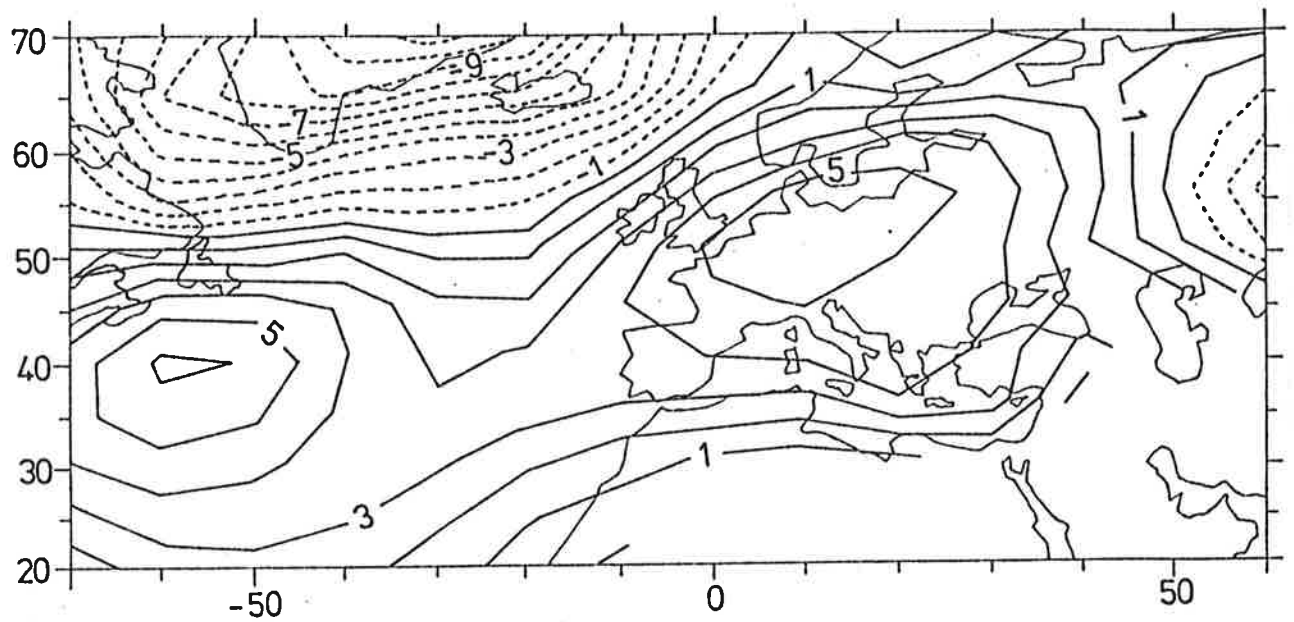
d)



1. The first two January EOFs of the Historical Sea Surface temperature (HSST: [19] Höflich, 1972). After Glowienka-Hense (1987). (a) EOF1 (16%); (b) EOF2 (9%); pattern of EOF's are normalized to have an absolute maximum value of 10, contour lines are drawn in subjectively for better visualization (c) time amplitude of EOF1; (d) time amplitude of EOF2.



2. Observed air temperature anomaly in January at Funchal (Madeira). After the World Meteorological Station Climatology. According to Jones et al (1985) the time series does not suffer from inhomogeneities. Dashed: raw data; continuous line: 10 year running mean. Units: °C.



3. Significant and recurrent signal in the difference between the observed air pressure decadal means 1904-13 and 1951-60. Units: hPa, contour interval 1 hPa. Negative anomalies are dashed. (After Glowienka-Hense, 1987).

1.2. GENERAL APPROACH

A first attempt to find an answer to the above questions through the help of a model study is reported in this paper. Three extended GCM runs were performed, each using a different SST distribution in the Atlantic Ocean. One run was done with the model's standard SST that is typical for the 1970's and two runs with the distributions averaged for the above mentioned decades: 1903-14 and 1950-60. Because of computer time limitations the experiments are performed in the "permanent January mode". The first experiment is called "control", the other two "cold" and "warm".

The expected result is that the differences between the atmospheric circulation in the GCM experiments compare to the observed changes. Since the model used is not free from systematical errors, as is usual with this type of low resolution GCMs, the coincidence of the observations and of the GCM simulations will be in their broad patterns only.

It is well-known that in this type of GCM sensitivity experiments the signal is often masked by the strong "weather-noise" at mid-latitudes. Therefore, it is inappropriate to compare naively the observed decadal change and the mean simulated difference "cold minus warm". Instead the stochastic character of the random variable "January mean flow" has to be taken into account by testing the null hypothesis

- * The simulated patterns of the hemispheric winter circulation associated with anomalous low and high Atlantic SSTs are identical.

If such a statistical test yields the positive result of a nonzero signal (i.e. the rejection of the null hypothesis) the following questions regarding the physics of the signal have to be asked

- * Is the response statistically stable, i.e. is it associated with a large probability of appearance in individual January means?
- * What is the three dimensional structure of the signal?
- * Can we specify reduced models which allow us to understand the modelled changes in terms of simplifying physical theory?

The last question and the test of the null hypothesis mentioned above may conveniently be treated jointly: Since the random variable "January mean flow" is a vector random variable, a multivariate statistical test has to be used (Hassel-

mann, 1979). This may be done in terms of a series of tests (Barnett et al., 1981) using a hierarchy of "guess patterns" which are specified prior to the test without using information from the GCM experiments except the time mean fields. The GCM fields are projected onto the guess patterns and the test is done in the low dimensional subspace spanned by the guess patterns. The rejection of the null hypothesis is a statistical proof that the guess patterns are skillful to explain the model's response.

Studies which have used the guess pattern / hierarchy approach successfully have been published by Hannoschöck and Frankignoul (1985), Hense (1986), Storch and Kruse (1985), Frankignoul and Molin (1988a,b) and Lautenschlager et. al. (1988). They used primarily scale arguments to specify the guess patterns, i.e. surface spherical harmonics, or, with little success, the response of physical models linearized around a zonally symmetric basic state. In the present study, we use in addition to the problem independent surface spherical harmonics two physically motivated sets of guess patterns: the eigenfunctions of the barotropic vorticity equation linearized around the (zonally non-symmetric) mean state for explaining the anomalies in the upper troposphere and the eigenmodes of the advection-diffusion operator for the flow at 1000 hPa for explaining the temperature response of the layer 850/1000 hPa.

The question of the statistical stability of the response may be addressed by the concept of "recurrence analysis" (Storch and Zwiers, 1988; Zwiers and Storch, 1989). We use both the univariate "local" recurrence analysis and the pattern oriented multivariate "global" analysis.

After having found a significant "cold vs. warm" signal, it is an interesting question to ask if the signal depends linearly on the SST forcing. We may address this question by examining experiments "cold vs. control" and "warm vs. control" which operate with the same SST anomaly pattern. In the "cold vs. control" the intensity of the SST anomaly is strongly negative, and in the "warm. vs. control" it is moderately positive. The analyses of the "cold vs. control" and "warm vs. control" experiments are done in the same manner as the "cold vs. warm" analysis.

1.3. PURPOSE AND ORGANISATION OF THE STUDY

The purpose of the paper is threefold:

- * To demonstrate the consistency of observed changes in SST and SLP on decadal time scales, and to show that the observed SLP changes may partially be understood as atmospheric response to changing boundary conditions (SST).
- * To show the usefulness of reduced models to interpret the output of GCMs, which usually have as complex a behavior as the real atmosphere.
- * To study the linearity of the atmospheric response to large scale SST anomalies.

We do not consider in this paper two related questions: The abrupt change of temperature in the northern part of the North Atlantic (e.g., van Loon and Rogers, 1978; Rogers, 1985), and the slow increase of interannual variability from the beginning to the middle of the present century (van Loon and Madden, 1983). Our SST data set does not resolve the northern part of the North Atlantic so that information on SST in that area is not available. To consider the variance problem the horizontal resolution (T21) of the GCM is likely too coarse.

The paper is organized as follows: In Section 2 the GCM and the experiments with it are described; in Section 3 the general statistical approach is briefly summarized. The hierarchies of guess patterns, and their physical motivation, are presented in Section 4. The filtering of the statistically significant signal in the "cold vs. warm" experiment, its physical plausibility and its statistical stability are presented in Section 5. The linearity of the model's response to anomalous Atlantic SST is examined in Section 6. The physics of the identified signal are discussed in the final Section 7.

2. Data

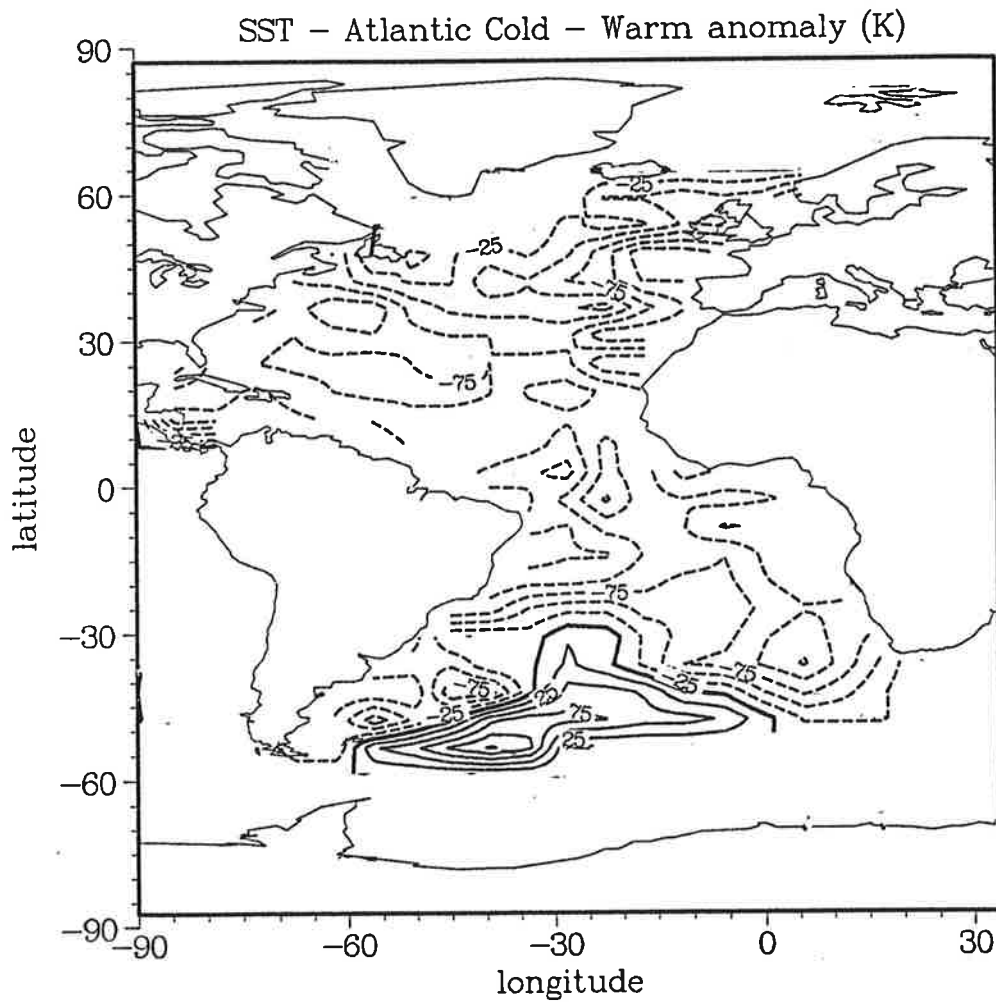
2.1. GCM EXPERIMENTS

The Hamburg version ("cycle 17") of the low resolution ECMWF T21 atmospheric GCM has been used to perform the experiments. For details of the structure, physics and general performance of the model see Fischer (1987) and Storch (1988). The perpetual January model runs were identical except for the prescribed SST field in the Atlantic between 70° N and 35° S. The first run integrated over 13 months ("control") using the model's standard SST climatology of Alexander and Mobley (1976) which is representative for the 1970's. The other two runs, named "warm" and "cold", were integrated over 24 months each, and used the January Atlantic SST averaged over the decades 1904-13 ("cold") and 1951-60 ("warm"). The first month in each run was considered as the spin-up phase needed by the model to reach its equilibrium.

The Atlantic SST fields were derived from the irregularly spaced HSST data set (Höflich, 1974) by an EOF analysis (Glowienka-Hense, 1987). EOFs and their amplitudes have been calculated from the January SST. The first two EOFs (Fig. 1) which explain 25% of the total interannual variance were considered relevant in describing the decadal changes. Therefore, the anomaly distribution described by the first two EOFs was reconstructed and, after decadal averaging, was used as an anomalous boundary condition. Fig. 4 shows the resulting difference between the "cold" and "warm" SST fields. There is an anomaly of 1.2°C in the tropical Atlantic and a structured anomaly between 1 and 0.33°C in the North Atlantic while a negative anomaly occurs in the South Atlantic. The "cold vs. control" ("warm vs. control") SST anomaly is roughly 2/3 (1/3) of the "cold vs. warm" anomaly. The SST anomaly patterns in the "cold vs. control" and "warm vs. control" experiments are identical, and are broadly similar to that in "cold vs. warm".

2.2. VERIFICATION DATA

No upper air data are available from the first decades of this century, so the verification of the GCM results is limited to sea level pressure (SLP), which is available to us for the period from 1881 to 1984. The different data sources and errors in this SLP data have been discussed by Glowienka (1985). Time series of station data (World Meteorological Station Climatology, available at NCAR) are



4. Decadal difference field of the Atlantic Ocean SST in January between 1904-1913 ("cold" experiment) and 1951-60 ("warm" experiment). The field is reconstructed from the first two January EOFs shown in Fig. 1. Units $10^{-2} \text{ }^{\circ}\text{C}$, contour interval 0.25°C .

available also, but are of limited value since the expected signal is a large scale one while the point measurements are likely to be influenced by local particularities and inhomogeneities.

3. Statistics

As mentioned in the Introduction we will use statistical techniques to evaluate the GCM response in a noisy environment. We consider the 30-day mean of a certain variable, e.g. streamfunction at 300 hPa or sea level pressure, as a random variable. That is, each 30-day mean obtained from the three runs, control, warm and cold, is considered to be a random sample of a random vector variable. These samples may be used to test whether the data contradict the null hypothesis of a zero signal (Sec. 3.1) and to estimate the level of global or local recurrence (Sec. 3.2). The (multivariate) significance test and the estimation of the level of recurrence will be done in a hierarchy (Sec. 4).

3.1. SIGNIFICANCE TEST

The null hypothesis to be tested is

$$H_0 : \mu_i = \mu_j \quad (3.1)$$

where μ_i is the expectation of the vector random variable x_i . The index i (and j) identifies the experiment, i.e. the cold, warm or control experiment. (3.1) may be tested conveniently by the Hotelling T^2 statistic if one assumes that the underlying ensemble is a multivariate normal distributed one (e.g., Hannoschöck and Frankignoul (1985) or Hense (1986)):

$$T^2 = \frac{n_i n_j}{n_i + n_j} D^2 \quad (3.2)$$

with

$$D^2 = (\bar{x}_i - \bar{x}_j)^t S^{-1} (\bar{x}_i - \bar{x}_j) \quad (3.3)$$

Here, the sample mean of experiment i is denoted by \bar{x}_i . S is the pooled estimate of the variance/covariance matrix Σ , and n_i the number of independent samples available from experiment i . To get an invertible S the dimension of the random variable, d , has to be smaller than the total number of available independent samples, $n_i + n_j - 2$.

If H_0 is true the function

$$F = \frac{n_i + n_j - d - 1}{d(n_i + n_j - 2)} T^2 \quad (3.4)$$

is Fisher-F distributed with d and $n_i + n_j - d - 1$ degrees of freedom: If F exceeds the $(1 - \alpha)$ quantile of the Fisher-F distribution, H_0 may be rejected at a risk of α . That is the probability to observe such a large F by chance if $\mu_i = \mu_j$ is less than α .

3.2. ESTIMATION OF THE LEVEL OF RECURRENCE

The rejection of the null hypothesis H_0 is equivalent to the acceptance of the alternative hypothesis " $\mu_i \neq \mu_j$ ". It does not indicate if the signal, i.e. the difference $\mu_i - \mu_j$, is large or small. In fact the power of the Hotelling test depends on the number of available samples, $n_i + n_j$: the more samples the better the chances to detect a nonzero signal. In other words: "Significance" is in part a property of the considered random variables, but also depends on the sample size, which has nothing to do with the physical problem under consideration but is a factor of the experimental design (Fig. 5a).

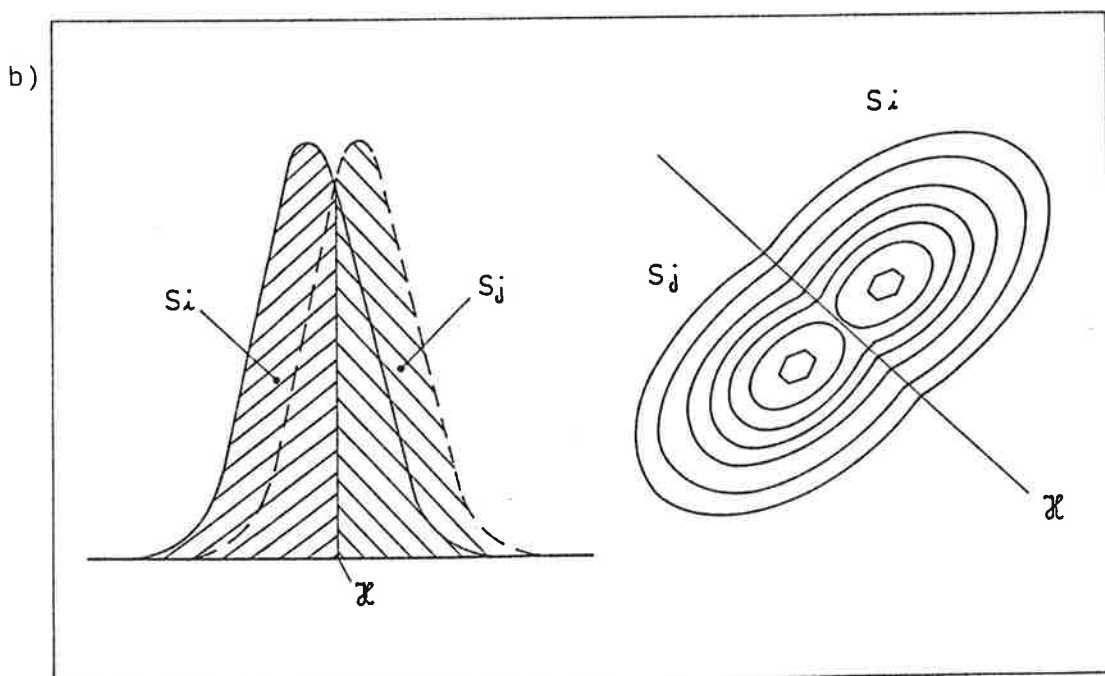
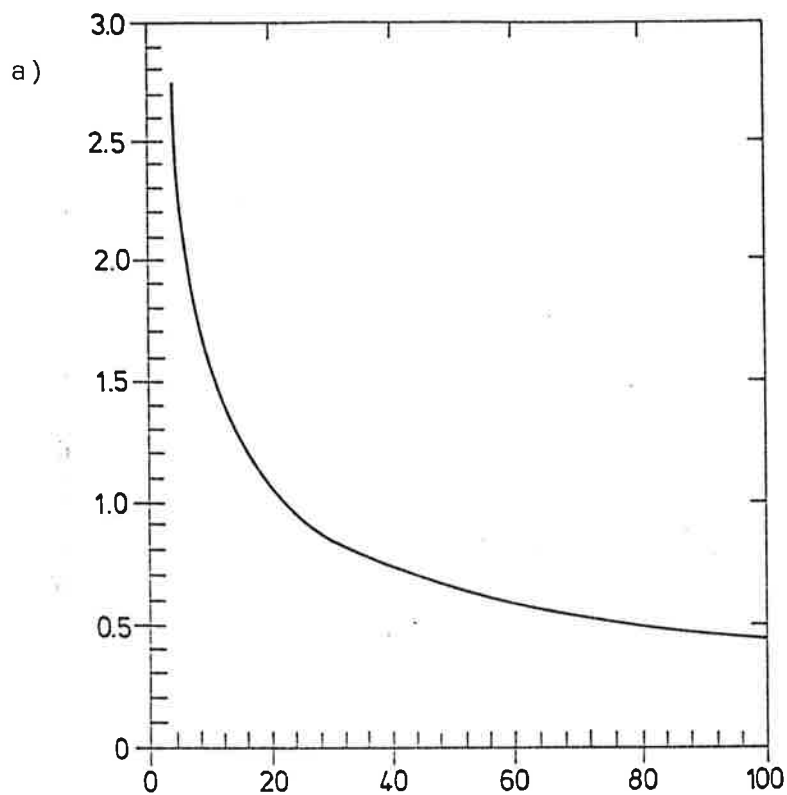
If the considered random variables, x_i and x_j , are univariate and Gaussian, another view of the problem is the following. The alternative hypothesis " $\mu_i = \mu_j$ is wrong" is equivalent to the probability statement

$$P(x_j > \bar{x}_i) > q \quad (3.5)$$

The probability q will be large if the separation of the two variables is large, i.e. if the signal $\mu_i - \mu_j$ is physically significant. A q close to 50% is indicative that the difference is not relevant. If, however, q is, say 51% the test will reject H_0 if the sample size is large enough. That is, statistical significance is a necessary but not sufficient condition for physical significance.

This somewhat unsatisfactory situation may be overcome by "recurrence analysis" (Storch and Zwiers (1988) and Zwiers and Storch (1989)). Using Multivariate Discriminant Analysis it is possible to define a $(d - 1)$ dimensional hyperplane \mathcal{H} which divides the whole R^d in two subsets S_i and S_j such that

$$P(x_j \in S_i) = P(x_i \in S_j) \leq 1 - p \quad (3.6)$$



5. On the concept of recurrence. (a) Minimum difference of means, in units of standard deviations, which is identified by a t-test with probability of at least 90%, if the sample size of both ensembles increases (horizontal axis). (b) Schematic diagrams to illustrate the subdivision of the d -dimensional space into two complementary sets, S_i and S_j with $S_i \cup S_j = R^d$. Left: $d = 1$, the curves show the probability densities. The $d - 1 = 0$ dimensional hyperplane \mathcal{H} is a point on the horizontal axis. Right: $d = 2$, contour plot of the probability densities. The 1-dimensional hyperplane \mathcal{H} is the straight line. (After Storch and Zwiers (1988) and Zwiers and Storch (1988).)

(see Fig. 5b). Since $S_i \cup S_j = R^d$, (3.6) is equivalent to $P(x_j \in S_j) = P(x_i \in S_i) = p$. If p is large (or small) the separation of the probability densities of the two random variables x_i and x_j is large, and if p is close to 50% the separation is small.

In the present paper we estimate the level of recurrence "globally" in the low dimensional subspace used for the significance test, and "locally" at each grid point, after having found significantly nonzero signals with the Hotelling test. If we suppose that the two random variables x_i and x_j are normally distributed with identical covariance matrix, $x_i = N(\mu_i, \Sigma)$ and $x_j = N(\mu_j, \Sigma)$, the level of recurrence p may conveniently be estimated using the "OS-method" (Zwiers and Storch (1989); Page (1985); Okamoto (1963)):

$$1 - p = \operatorname{erf}\left(-\frac{DS}{2}\right) + \frac{\phi\left(-\frac{DS}{2}\right)}{(n_i + n_j - 2)} \left(\frac{DS}{16} \left(\frac{(n_i + n_j - 1)^2 - 1}{n_i n_j} \right) - \frac{d-1}{4DS} \left(\frac{(n_i - 3n_j)(n_i + n_j - 2)}{n_i n_j} - DS^2 \right) \right) \quad (3.7)$$

where ϕ denotes the Gaussian probability density function, $\operatorname{erf}(x)$ the error function, and DS^2 the "shrunk D":

$$DS^2 = \frac{(n_i + n_j - d - 3)}{(n_i + n_j - 2)} D^2 \quad (3.8)$$

In the univariate case (3.8) is the difference of sample means measured in units of the estimated standard deviation. A level of $p = 84\%$ corresponds to the well known "2 σ " rule of thumb: The difference between the two means is larger than twice the standard deviation. $p = (60, 66, 84)\%$ in (3.6) corresponds to $q = (70, 80, 98)\%$ in (3.5) (Storch and Zwiers, 1988, their Table 2).

The estimation of the level of recurrence may be done without any reference to the significance of the distance of the climates, D , and any nonzero D will give a recurrence different from 0.5. But from the arguments of the preceding section it is clear that a certain level of recurrence is only meaningful after having rejected the null hypothesis of a zero signal with a sufficiently small risk.

4. Guess Patterns and Hierarchies of Test Models

The dimension of the vectors x_i and x_j considered in this study is the number of gridpoints on the northern hemisphere, i.e. of the order of 10^3 . On the other hand, the numbers of independent samples, n_i and n_j , are of the order of 30 (see Chapter 5 for details). Therefore the sample covariance matrix in grid point space can not be inverted and the test statistic D^2 can not be calculated. To overcome this problem the data are projected into a low-dimensional subspace with dimension $d \leq 30$. The subspace is specified by a linear basis $\{g_1, \dots, g_d\}$. The high-dimensional vectors, g_k , which can be displayed as maps covering the whole northern hemisphere, are called guess patterns.

There are two advantages of the guess pattern concept which was suggested by Hasselmann (1979). First, it is possible to increase the power of the test, i.e. the probability to confidently identify a signal, by selecting patterns which a-priori are known or are believed to represent the signal. Second, when using indexed guesses the analysis may be done using the method of hierarchical ordering of certain a-priori chosen test models (Barnett et al., 1981): The test is done sequentially on subspaces of increasing dimension $\{g_1, \dots, g_k\}$, $k \leq d$. In this way for each k one "model" is fitted to the data, namely the projection of the full signal on the subspace spanned by the first k guesses.

If the null hypothesis, it depends now on the number k and is thus labelled as H_0^k , is rejected for certain k 's at an error level level of 10% we chose as the best model the one with maximum k and an estimated level of recurrence $p \simeq 80\%$.

There are essentially three strategies to derive sequences of useful guess patterns (Storch, 1987):

- * A-priori information on the expected signal. This information may originate from independent observations or numerical experiments. In our case no such information is readily available.
- * Patterns which are known to be effective in representing data but which are not specifically related to the problem under consideration. In this study we use Surface Spherical Harmonics (Sec. 4.1). The advantage of this specific hierarchy is that it may be applied without any restrictions to all horizontal fields generated by the GCM.
- * Patterns obtained from simplified theory which is supposed to describe the

considered problem to some extent. We use two simple models to anticipate the GCM experiment signals: the eigenfunctions of the linearized barotropic vorticity equation (Sec. 4.2) and the eigenmodes of the advection - diffusion operator for the flow at 1000 hPa (Sec. 4.3).

4.1. S-HIERARCHY: SCALE DEPENDENT HIERARCHY OF SURFACE SPHERICAL HARMONICS

The surface spherical harmonics Y_l^m which formally are defined as the eigenfunctions of the Laplacian on the sphere are known to represent data on a sphere in an efficient manner. They may conveniently be indexed by the "total" wave number l and the zonal wave number m . l is indicative of the horizontal scale of the function and m of the zonal scale. The scales decrease with increasing indices l and m .

From the scale of the anomalous forcing, namely the Atlantic SST anomaly shown in Fig. 4, we anticipate that the signal will be a larger scale one. Therefore the "S-hierarchy" of spherical harmonics is specified by the indices l and m (Hannoschöck and Frankignoul (1985), Hense (1986)): the ordering is done according to l and, at a fixed l , with increasing zonal wavenumber m ($\leq l$). The ordering will result in a scale dependent hierarchy with the large scale modes being tested first.

Considering hemispheric fields only we limit the analysis to either odd (streamfunction) or even (sea level pressure, temperature) modes. A total hierarchy number of 21 (28) modes corresponds to a T6 (T7) truncation for an antisymmetric field with each mode of nonzero zonal wave number adding two degrees of freedom. Since it is likely that the global means of the analysed variables are unchanged the superrotation mode Y_1^0 is disregarded.

4.2. B-HIERARCHY: BAROTROPIC NORMAL MODES

The quasigeostrophic barotropic vorticity equation is supposed to model small disturbances of the midlatitude atmospheric flow to first order.

$$\frac{\partial}{\partial t} \nabla^2 \Psi + J(\Psi, \nabla^2 \Psi + f) = -\alpha \nabla^2 \Psi + F \quad (4.1)$$

where Ψ is the geostrophic streamfunction, $J(a, b)$ is the Jacobian operator and F_i represents all processes not represented by the barotropic model.

We use the eigenvectors of a linearized version of (4.1) to establish one set of problem-dependent guess patterns. In contrast to the S-hierarchy this set of patterns has the advantage of providing physically based suggestions for the mechanism of circulation changes. Due to the barotropy it has the disadvantage of being limited to the non-tropical middle troposphere.

To derive the eigenvectors we follow Simmons et al (1983) and Branstator (1985 a,b). After writing the state Ψ as a sum of a mean state $\bar{\Psi}$ and a disturbance $\Psi'(t)$, $\Psi = \bar{\Psi} + \Psi'$, and after linearization the following equation is obtained:

$$\frac{\partial}{\partial t} \Psi' + M[\bar{\Psi}] \Psi' = F' \quad (4.2)$$

The matrix M arises from the Jacobians and the Ekman damping in (4.1) and is readily calculated using pseudo-spectral methods as suggested by Simmons et al. (1983). The notation $M[\bar{\Psi}]$ indicates that the matrix M depends on the mean state $\bar{\Psi}$.

The matrix M has (complex) eigenvalues λ_j and eigenvectors e_j . Each state Ψ' and F' may be expressed by the eigenvectors.

$$\begin{aligned} \Psi' &= \sum_j a_j \cdot e_j \\ F' &= \sum_j f_j \cdot e_j \end{aligned} \quad (4.3)$$

with the coefficients

$$\begin{aligned} a_j &= d_j^t \cdot \Psi' / d_j^t \cdot e_j \\ f_j &= d_j^t \cdot F' / d_j^t \cdot e_j \end{aligned} \quad (4.4)$$

The vectors d_j^t are the adjoint vectors of the e_j (i.e., $M^t d_j = \lambda_j^* d_j$) which form a biorthogonal basis such that $d_j^t \cdot e_i = 0$ if $i \neq j$. Inserting these expressions into (4.2) we find as the stationary response Ψ' to the anomalous forcing F' .

$$\Psi' = \sum_j \frac{1}{\lambda_j} f_j \cdot e_j \quad (4.5)$$

The response is stationary if the eigenvalues have positive real parts. It turned out that a damping rate of $\alpha = 1/10 \text{ days}^{-1}$ was sufficient to guarantee that all eigenvalues had positive real parts.

In view of the above consideration it appears reasonable to use the eigenvectors e_j to guess the response of the GCM experiment. To do so the eigenanalysis is done in the R11 (antisymmetric modes only) spectral space. The mean state $\bar{\Psi}$ is specified by the geostrophic streamfunction in 300 hPa.

If we define $\bar{\Psi}$ to be the average of two simulations (e.g. cold and warm or warm and control) (4.2) is formally equivalent to an anomaly general circulation model (Navarro and Miyakoda, 1988; Schneider, 1988). If $\bar{\Psi}$ is the average of only one experiment (4.2) is formally a disturbance GCM experiment with the chosen basic flow being disturbed by the anomalous boundary conditions.

The remaining question is how to define an adequate hierarchy. The most important patterns are associated with large coefficients $a_j = \frac{f_j}{\lambda_j}$. Clearly the optimal choice of the pattern would be obtained by ordering the patterns by the weights: $\frac{f_1}{\lambda_1} > \frac{f_2}{\lambda_2} > \dots$. Unfortunately, the forcing is not known: The connection between anomalous SST and anomalous vorticity forcing F' at 300 hPa is highly nonlinear and complex. Another ordering would be $\|d_1\| > \|d_2\| > \dots$: If d_j is large then one can expect f_j to be large also. We tried this approach and found it to be not successful.

The finally chosen ordering

$$\|\lambda_1\| < \|\lambda_2\| < \dots \quad (4.6)$$

is based almost solely on the imaginary (frequency) part of the eigenvalue. Those gravest modes are anticipated to be most probably affected by a stationary forcing.

Thus the barotropic normal mode "B-hierarchy" is defined by the sequence of eigenmodes of a specified basic flow $\bar{\Psi}$ ordered according to the modulus of their respective eigenvalues. This hierarchy is similar to the one used by Hannoschöck and Frankignoul (1985) but differs in one essential aspect: They used a zonally averaged mean state whereas we use a zonally asymmetric mean state.

4.2.1. HIERARCHY A: NORMAL MODES OF THE TEMPERATURE ADVECTION MODEL

Egger (1977) suggested that the atmospheric response to midlatitude SST anomalies is mostly confined to the lower troposphere, and that the additional heating Q is balanced mainly by horizontal advection and an diffusive eddy transport:

$$\frac{\partial}{\partial t}T = -J(\Psi, T) + \epsilon \nabla^2 T + Q \quad (4.7)$$

A similar concept is that of the "advective limit" proposed by Webster (1981). Defining as above a mean \bar{T} and an anomaly T' we get the following model for the anomaly

$$\frac{\partial}{\partial t}T' = -J(\bar{\Psi}, T') - J(\Psi', \bar{T}) + \epsilon \nabla^2 T' + Q' \quad (4.8)$$

Since no a-priori information on $J(\Psi', \bar{T})$ is available this term has to be dropped. The model (4.8) can not explain stationary solutions for the hemispheric averaged temperature anomaly unless the area averaged anomalous heating is zero neglecting heat fluxes across the equator. Consequently we have to drop again the Ψ_1^0 mode. Then, (4.8) is formally identical to (4.2) and the guess patterns are chosen to be the eigenvectors of a matrix $M[\bar{\Psi}]$ which is derived from the advection and diffusion terms in (4.8). The same principle which led to the B hierarchy is used to define the A hierarchy, i.e. the modes are ordered according to the modulus of the eigenvalues.

The mean flow at 1000 hPa is used to specify $\bar{\Psi}$. Diffusion coefficients $\epsilon > 100m^2/sec$ were large enough for all eigenvalues to have positive real parts.

5. Analysis of the "warm vs. cold" experiment

5.1. TECHNICAL DETAILS

The GCM output variables which were investigated were daily values of the spherical harmonic coefficients of the geopotential height at 300, 500 and 850 and 1000 hPa, the last one derived from SLP. With the help of the linear balance equation the geostrophic streamfunction was derived. The low level temperature was approximated by the 850 hPa over 1000 hPa thickness: $T' \propto (\Psi(850hPa) - \Psi(1000hPa)) = \Delta_{850,1000}\Psi'$.

From these daily values, geostrophic streamfunction and lower level temperature, 30-day averages were formed. The first 30 days were omitted to avoid initial transients. Adjacent 30-day periods were separated by 10-day periods in order to obtain approximately independent realisations of a mean January climate.

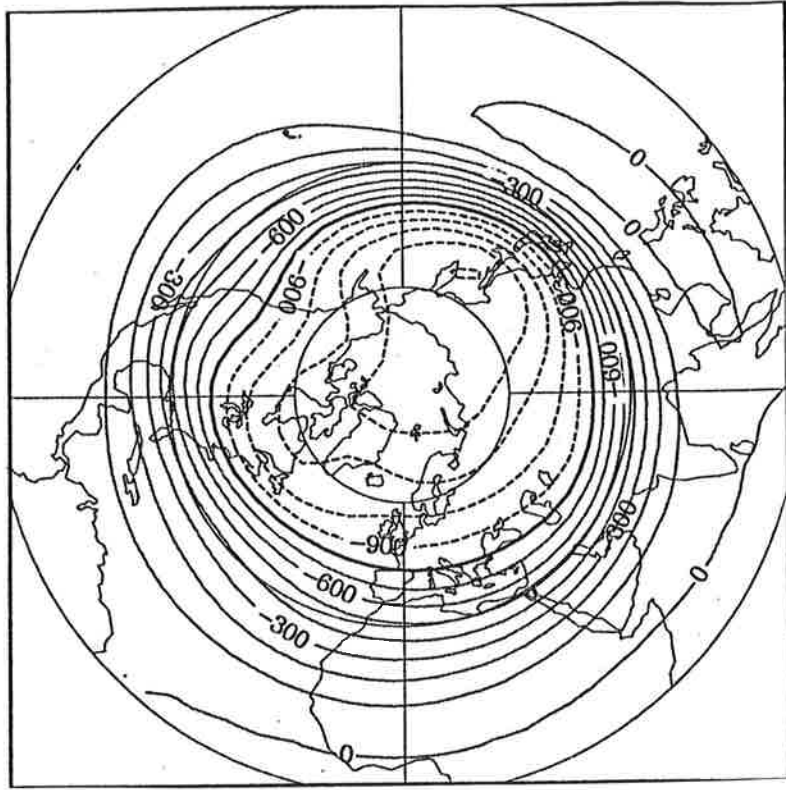
This procedure resulted in two sets of size 17 of "warm" and "cold" monthly means which form the samples on which to perform the statistical analysis in the three hierarchies, S, B and A. For the barotropic mode B-hierarchy the mean flow at 300 hPa, averaged over the warm and the cold experiment, is used (Fig. 6a). Similarly, the mean streamfunction at 1000 hPa, averaged over the two experiments, serves as $\bar{\Psi}$ in the A-hierarchy (Fig. 6b).

Once a significant model is identified in the hierarchy (maximum number of parameters with risk less than 10% and level of recurrence $> 80\%$; see Sec. 4) its mean difference is projected back into grid point space to obtain a statistically filtered version of the response. This will be called the significant and recurrent pattern. The multivariate analysis was performed in the low dimensional subspace spanned by the guess patterns. Therefore, the grid point representation of the significant and recurrent signal must not be interpreted locally. To allow for a regional assessment of the signal's statistical stability an additional local recurrence analysis is performed.

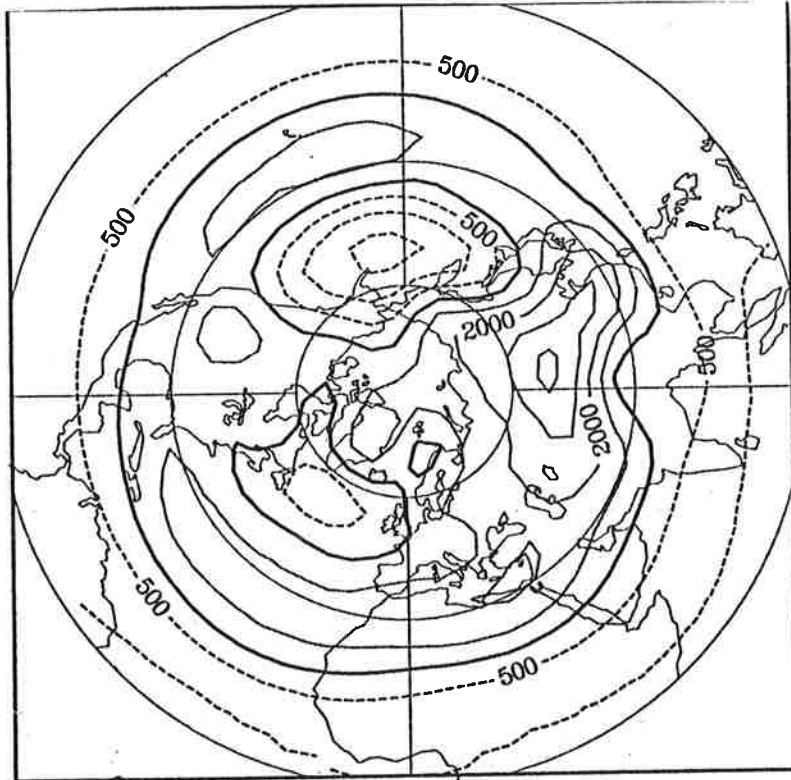
5.2. RESULTS

The results of the statistical analysis of the "cold vs. warm" experiment are summarized in Table 1.

a)



b)



6. Long term average geostrophic streamfunction in the warm and the cold experiment. (a) 300 hPa: the mean flow to derive the barotropic normal modes of the B hierarchy, units m^2/sec , contour interval $10^7 \text{ m}^2/\text{sec}$, (b) 1000 hPa: the mean flow to derive the temperature advection normal modes of the A hierarchy, units m^2/sec , contour interval $5.0 \cdot 10^6 \text{ m}^2/\text{sec}$

Table 1: Summary of the statistical analysis of the "cold vs. warm" experiment using the hierarchies S, B and A.

LH: Level of hierarchy which is identified as being significant and recurrent (= number of modes)

R: Risk = probability of equal means

LR: level of recurrence = probability to correctly classify one sample as being from the warm or the cold experiment.

EV: Part of the total signal's variance explained by the significant and recurrent signal (%).

"*****" indicates that the hierarchy is not applicable, "—" that no significant signal was identified, and (...) that the signal is significant but its estimated level of recurrence is less than 80%.

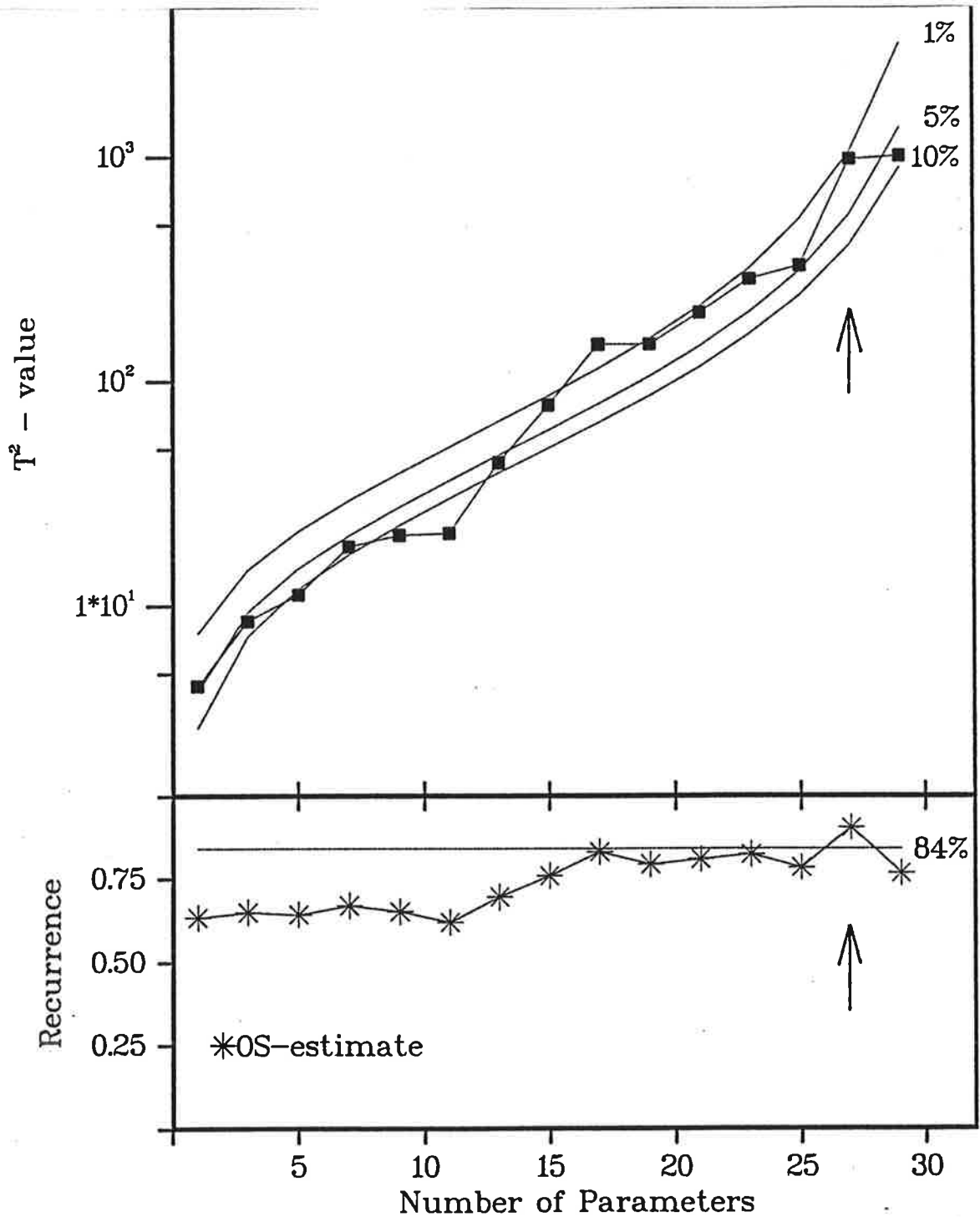
variable	hierarchy S				hierarchy B				hierarchy A			
	LH	R	LR	EV	LH	R	LR	EV	LH	R	LR	EV
streamfunction												
1000 hPa	23	5%	81%	75%	*****				*****			
850 hPa	(10	5%	70%	45%)	*****				*****			
500 hPa	(10	5%	70%	46%)	*****				*****			
300 hPa	7	1%	75%	55%	(11	5%	70%	45%)	*****			
850/1000 hPa layer												
temp.	12	10%	74%	51%	*****				27	5%	90%	46%

5.2.1. LOW LEVEL TEMPERATURE

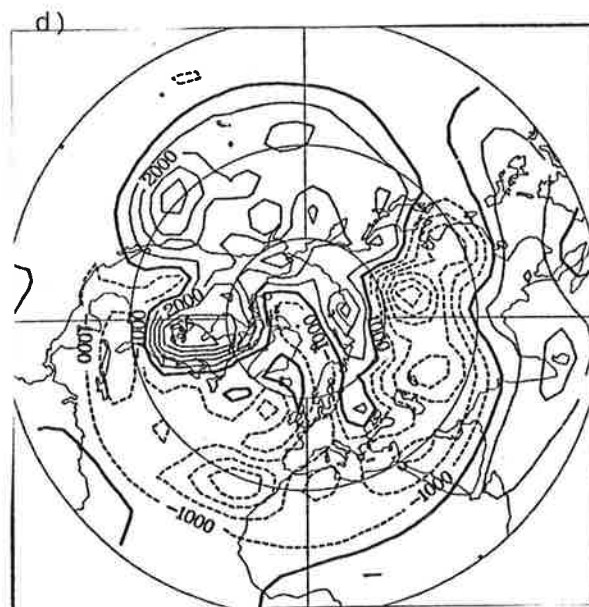
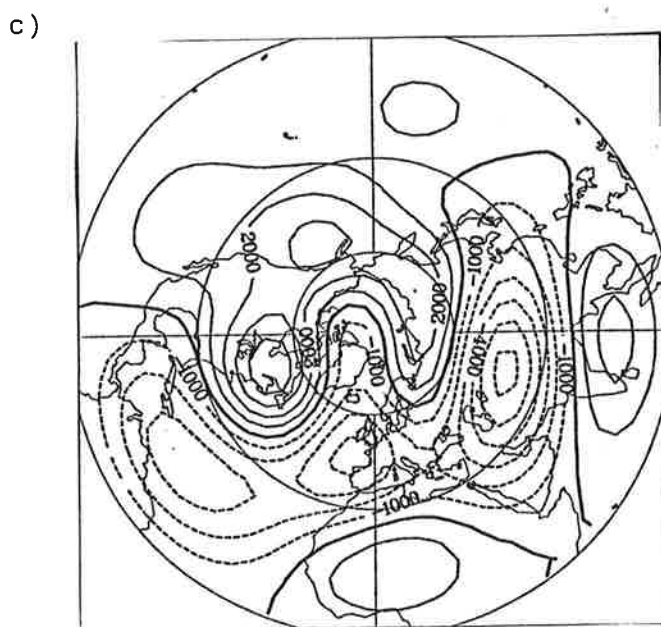
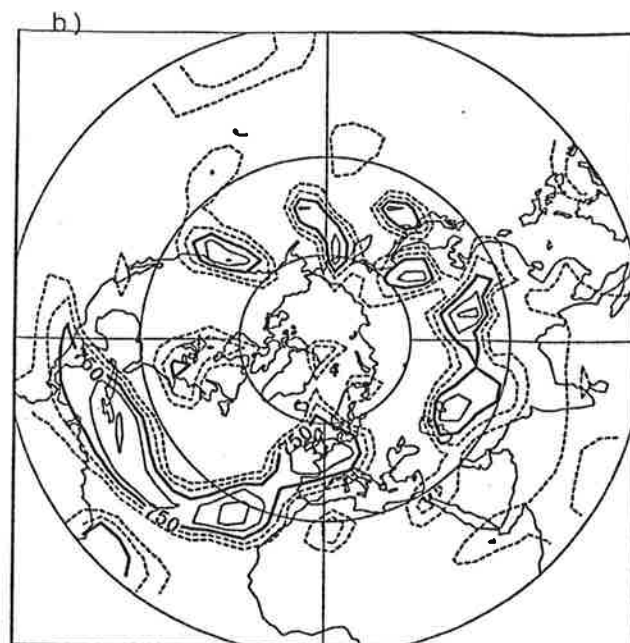
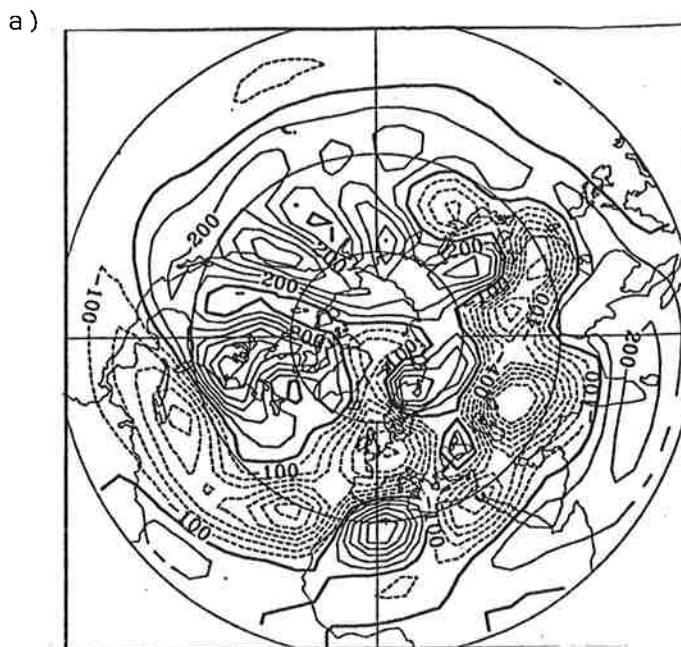
As an example, the risk of the statistical test and the estimated level of recurrence are displayed in Fig. 7 as a function of the level of the hierarchy for 850/1000 hPa layer temperature in the A-hierarchy. Only odd numbers of parameters enter the diagram because one stationary mode ($Im(\lambda_k) = 0$) contributes to the hierarchy with one degree of freedom whereas all other modes add two parameters each (see Simmons et al. (1983) and Branstator (1985 a,b)). The eventually chosen model has 27 parameters. At this number of parameters the risk of falsely rejecting the null hypothesis is less than 5% and the level of recurrence is clearly maximum. An alternate choice could have been 17 parameters yielding a model of less than 1% error level and 80% level of recurrence.

The 850/1000 hPa layer temperature $\Delta_{850,1000}\Psi$ contains a significant and recurrent signal in both applicable hierarchies A and S (see Table 1). In Fig. 8 the reconstructed A- and S signals are shown together with the full signal and the level of local recurrence. The A-signal describes much more detail than the S signal which is restricted to very large-scale guess patterns. The full signal is characterized by a general cooling of the western hemisphere (30W - 150E) and a warming in the eastern hemisphere. Additionally there are various small-scale features many of which reflect weather noise and random sampling. The same large-scale feature is present in the two filtered maps, also. The S and the A signals also correspond largely with respect to details. In the cold experiment, the lower troposphere over the eastern North Atlantic and most of midlatitude Eurasia was cooler than in the warm experiment. Simultaneously there is a positive anomaly over the midlatitude Pacific and North America, with a maximum situated over eastern Canada.

The high local recurrence levels indicate a stable temperature change over the eastern Atlantic and over Europe. The probability of negative temperature anomalies over the midlatitude Atlantic or Central Asia appearing in an individual January mean in another January simulation with "cold" Atlantic SST is estimated to be up to 85% or more when we compare it with the existing "warm" ensemble.



7. Test statistic T^2 (top) and estimate of recurrence (bottom) as a function of A-hierarchy parameters for the 850/1000 hPa layer temperature in the "cold vs. warm" experiment. The continuous lines in the top panel are the indicated error levels for T^2 if the null hypothesis holds. The arrow marks the model which was selected as being "significant and recurrent".



8. 850/1000 hPa layer temperature signal in the "cold vs. warm" experiment. (a) total difference field, units m^2/sec , contour interval 10^5 m^2/sec ; (b) level of local recurrence p , $p = 77$ (84)% corresponds to $q = 93$ (98)% in Storch and Zwiers (1988) and Eq. (3.5), units %, contour interval 5%; (c) "Significant and recurrent" signal in the S-hierarchy, contour interval as in (a); (d) "Significant and recurrent" signal in the A-hierarchy, contour interval as in (a).

5.2.2. STREAMFUNCTION

A significant and recurrent signal is identified in the S hierarchy at 1000 hPa and in 300 hPa (Table 1). The signals at 850 hPa and 500 hPa are significant at the 5% error level but the level of recurrence is only 70%. The same holds for the barotropic eigenmode hierarchy at 300 hPa where the recurrence level is always less than 70%. Therefore only the signals at 1000 and 300 hPa are shown in Fig. 9 and Fig. 10.

The S-filtered signal at 1000 hPa picks up roughly 75% of the total field variance of the raw signal "cold vs. warm". The S-reconstruction shown in Fig. 9c exhibits basically a wavenumber 1 response: a positive anomaly has developed over and downstream of the cooler Atlantic SST with opposite response for continuity reasons in the remaining part of the hemisphere. The local stability analysis (Fig. 9b) results in a fairly patchy pattern with maximum p values of 88%.

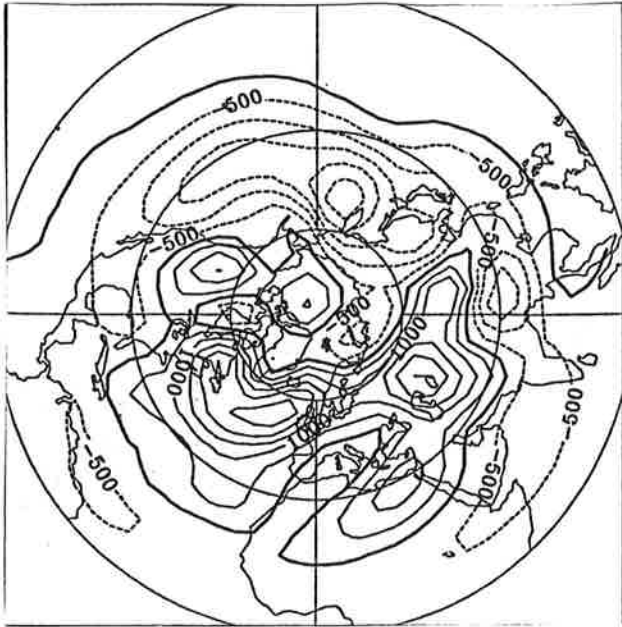
The low-level temperature and streamfunction anomaly are synoptically consistent. The anomalous anticyclonic flow over the North Atlantic is connected with a southeasterly wind anomaly in the western part of the ocean, advecting anomalously warm maritime air masses to the cold land while a northerly wind anomaly in the European sector leads to negative temperature anomalies in that area.

The upper level signal (Fig. 10) at 300 hPa is considerably different from the low level signal. In the cold simulation a dipole over North America indicates a reduced jet over the east coast of the U.S. and an intensified zonal flow over the Atlantic. At the same time the Asian jet appears to be strengthened in the cold run. The univariate recurrence analysis suggests that both features are stable, in particular with respect to the meridional gradient over North America ($q = 85\%$).

5.3. DISCUSSION

In the Introduction we questioned if the observed decadal changes of SST were real and, if so, whether the simultaneously observed changes of the atmospheric circulation may be understood in part as an atmospheric response to the altered Atlantic SST. To tentatively answer these questions on the basis of our experiment we have to compare the model results with observations. For practical reasons, i.e. data availability, we have to limit this verification to SLP or the 1000 hPa stream function.

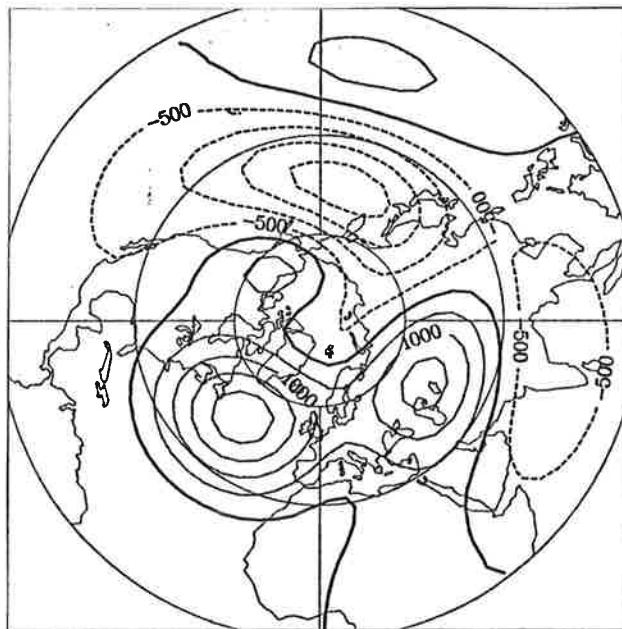
a)



b)

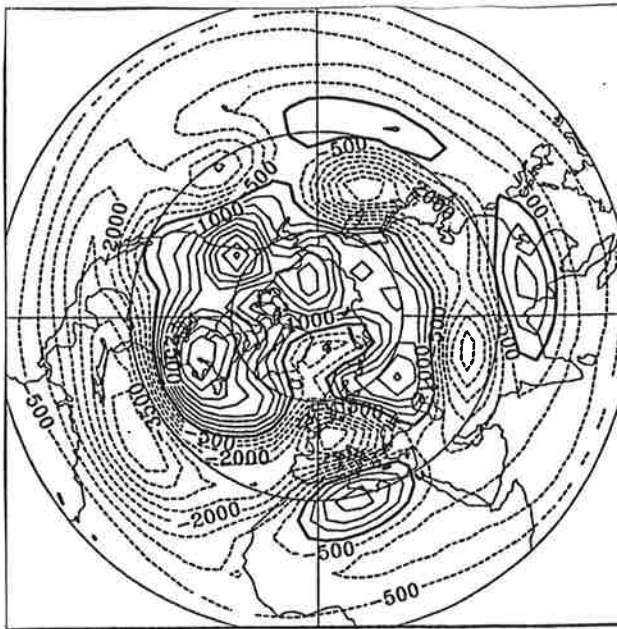


c)

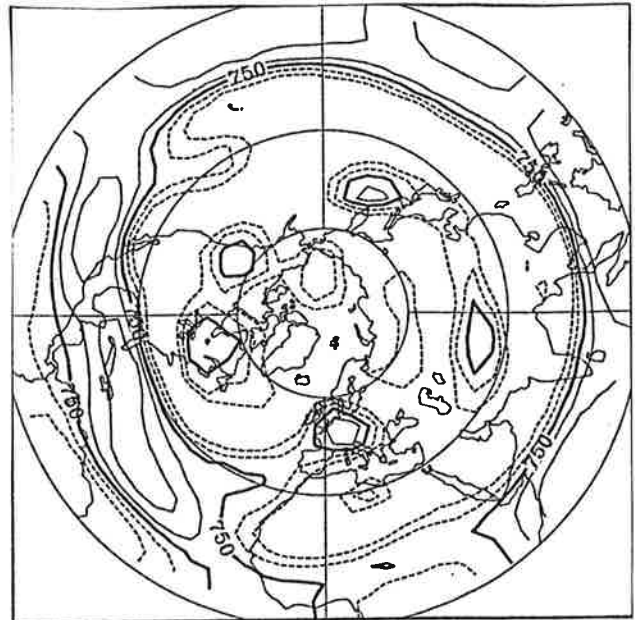


9. 1000 hPa streamfunction signal in the "cold vs. warm" experiment. (a) total difference field, units m^2/sec , contour interval $5.0 \cdot 10^5 \text{ m}^2/\text{sec}$; (b) level of local recurrence p , $p = 77$ (85)% corresponds to $q = 93$ (98)% in Storch and Zwiers (1988) and Eq.(3.5), units %, contour interval 5%; (c) "Significant and recurrent" signal in the S-hierarchy, contour interval as in (a).

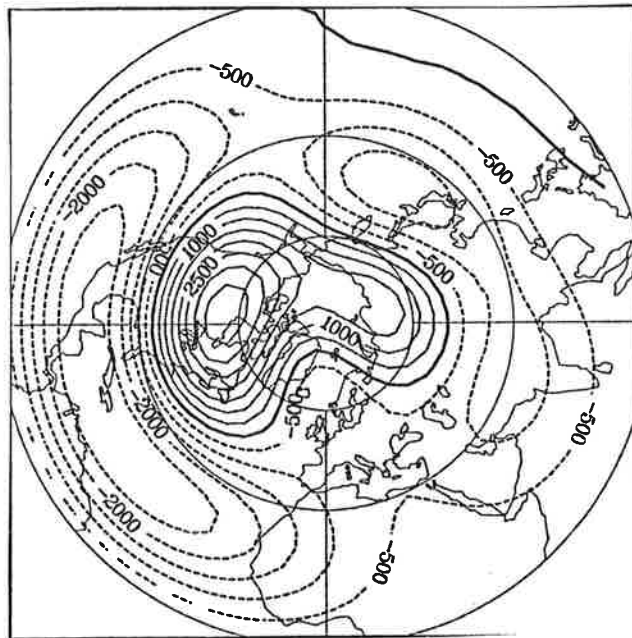
a)



b)



c)



10. 300 hPa streamfunction signal in the "cold vs. warm" experiment. (a) total difference field, units m^2/sec , contour interval $5.0 \cdot 10^5 m^2/sec$; (b) level of local recurrence p , $p = 77$ (85)% corresponds to $q = 93$ (95)% in Storch and Zwiers (1988) and Eq.(3.5), units %, contour interval 5%; (c) "Significant and recurrent" signal in the S-hierarchy, contour interval as in (a).

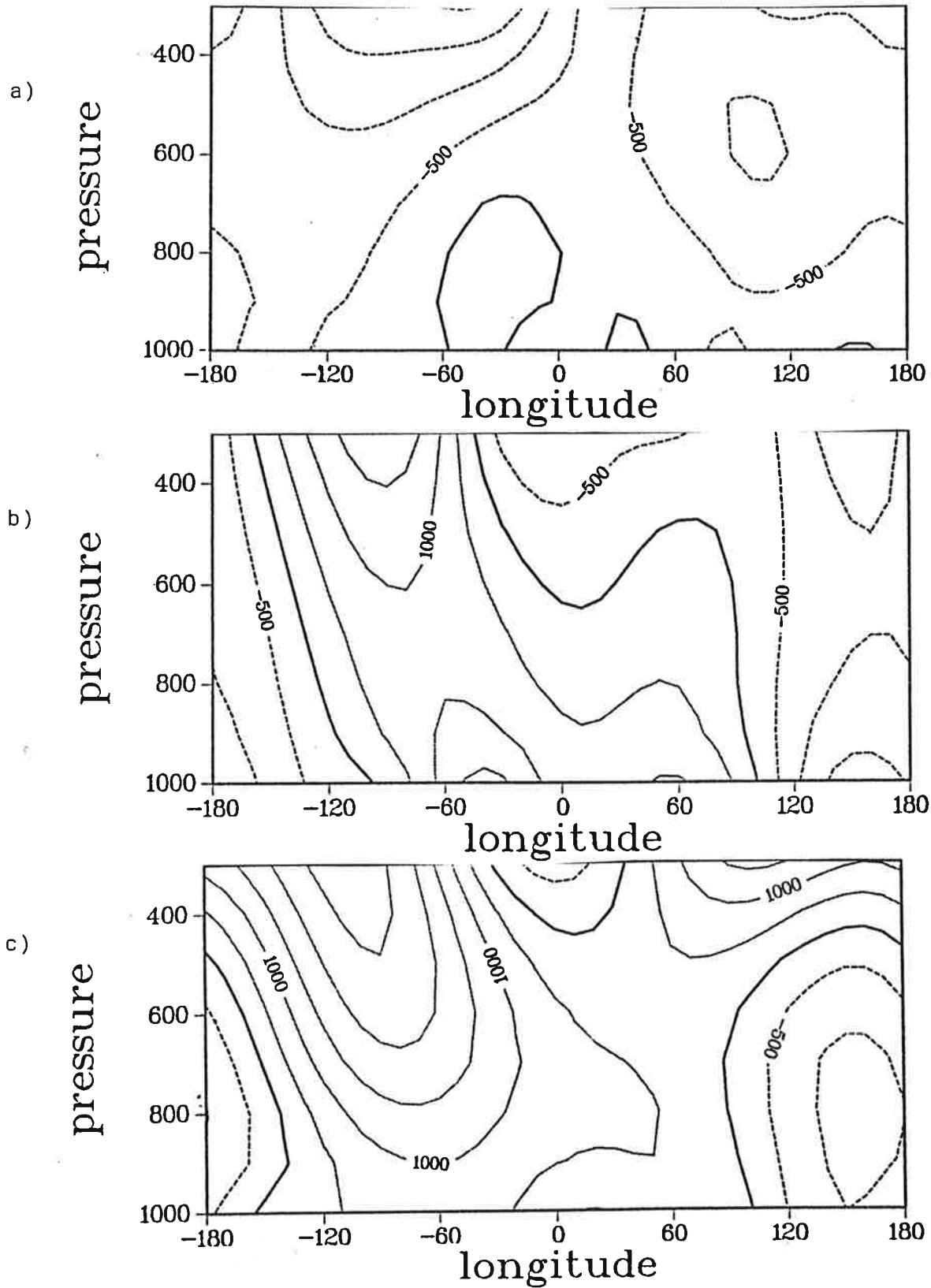
From the SLP observations a significant and recurrent pattern (5% and 80%) can be established for the difference in the average January fields between 1904-13 and 1951-60 (Fig. 3). This is based on the same methods as presented above except that we used as a hierarchy the regional EOFs of the Atlantic - European sector estimated from all January fields between 1881 and 1984. Comparison with the simulated Ψ_{1000} pattern (Fig. 9) yields a gross similarity: in both maps there are two maxima over the midlatitude Atlantic and Western Europe, and anomalous westward flow north of approximately 60°N . A more detailed comparison reveals that the simulated pattern are somewhat shifted relative to the observed mean pattern by about 30° to 50° of longitude to the east, and by about 10° to 20° to the north.

When comparing the simulated field and the observed changes we have to keep in mind that the model is not perfect in reproducing climatology, in the Atlantic sector and with respect to the North Atlantic Oscillation (Glowienka-Hense, 1988). In view of this limitation, we conclude that the GCM is largely reproducing the observed atmospheric changes as a response to modified Atlantic SST, at least in terms of low level circulation and temperature.

We anticipated two more questions to be asked if a significant signal would be identified, namely on the signal's three dimensional structure and the possibility to explain part of the signal in terms of simplified theory.

The statistical analysis identified stable signals in the S-hierarchy at 1000 and 300 hPa (Fig. 9c and Fig. 10c) and less well defined signals at 500 and 850 hPa (not shown). Fig. 11 displays the meridional average of the S-filtered streamfunction anomalies within three zonal belts: low, middle and high latitudes. The structure of the signal at low levels differs strongly from that at upper levels. The near surface level anomalies, between 850 and 1000 hPa, rarely exceed 10^6 m^2/sec in the Atlantic - European region and the response in that region (Fig. 11b) appears to be local and shallow. Within the high latitude strip where no local forcing exists the response is restricted to the upper layers. The upper tropospheric response, however, appears to be out-of-phase or unrelated to the surface anomalies. This is most pronounced in the low latitude belt but also visible in the middle and high latitude strip with the exception of the Pacific region.

Thus the vertical structure of the signal in the extratropics can be described as a two layer response of the lower troposphere (1000 and 850 hPa) against the



11. Meridional average, as a function of longitude and height, of the S-filtered streamfunction anomalies in the "cold vs. warm" experiment. units m^2/sec , contour interval $5.0 \cdot 10^5 \text{ m}^2/\text{sec}$; (a) $0^\circ\text{N} - 30^\circ\text{N}$; (b) $30^\circ\text{N} - 60^\circ\text{N}$; (c) $60^\circ\text{N} - 90^\circ\text{N}$.

upper troposphere (500 and 300 hPa). We suggest two possible explanations for this result.

- * The "baroclinic" hypothesis: The additional local heating from the ocean excites a baroclinic atmospheric response in which upper and lower levels are coupled.
- * The "two mechanisms" hypothesis: At lower levels the extratropical anomalies are the local response to the thermal changes whereas at upper levels we see the remote response to tropical flow anomalies, upper and lower layer tend to be decoupled at midlatitudes.

We favor the "two mechanisms" hypothesis for several reasons. First, the notion of a baroclinic response to extratropical SST anomalies would conflict with many GCM experiments (e.g., Rowntree 1979), with Barnett et al.'s finding (1984) that Atlantic SST anomalies tend to excite only local and regional downstream atmospheric responses, and also with the notion of the "advective limit" (Webster, 1981). The latter is supported by the success of the A-hierarchy based on the eigenmodes of the low level temperature advection equation: about one half of the low level temperature response can be explained by the linear advection and diffusion of the anomalous heating, a result in line with Egger's (1977).

The failure of the B-hierarchy (Table 1) was fairly unexpected for us, especially in view of the result presented in the next chapter. There appear to be several possible reasons for this:

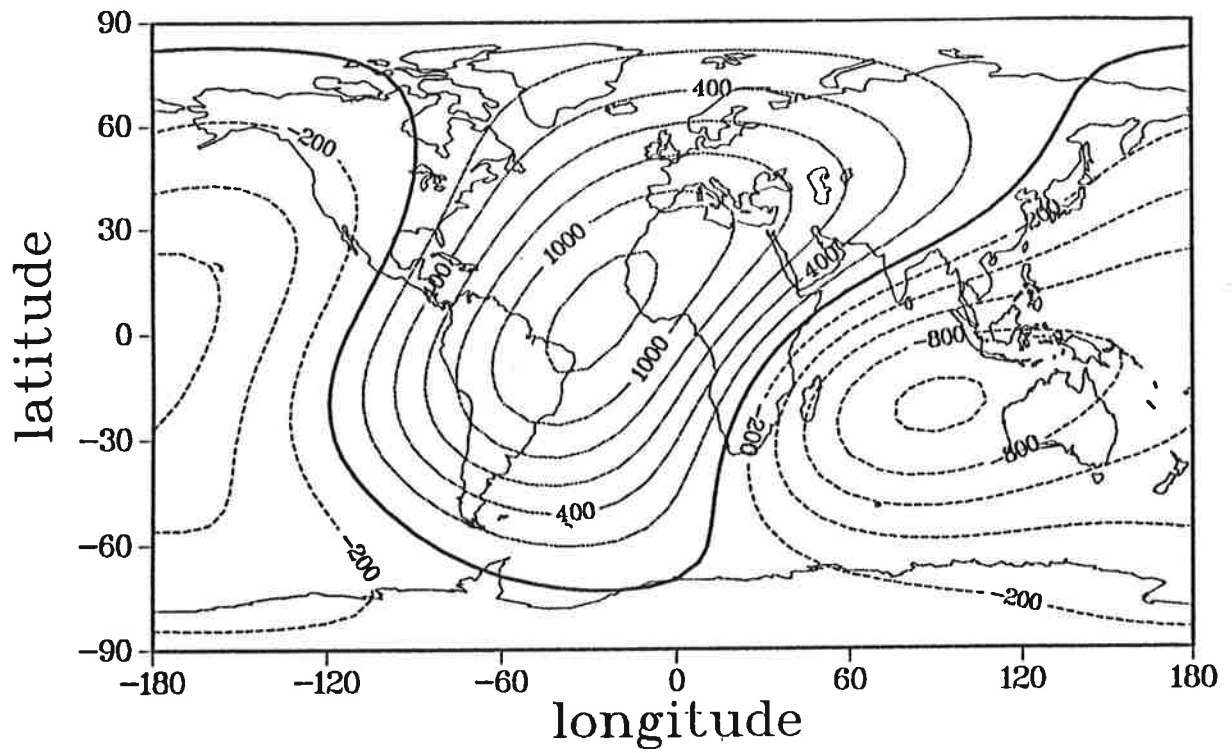
- * The basic ansatz leading to the B hierarchy is an inadequate description of the governing physics, i.e. the notion of the response being a small disturbance is not applicable. In the next chapter we will see that this is probably true.
- * The normal modes, and thus the result of the statistical analysis, depend strongly on the choice of the model's parameters such as reported in Frankignoul and Molin (1988b). A sensitivity analysis leads us to reject this hypothesis. Normal modes were derived using mean flows from all combinations, warm, cold and control. The eigenmodes, and the statistical results as well, are only marginally sensitive to the variations of the average flow which may be understood as an a-posteriori justification of the linearization.
- * The hemispheric formulation of the barotropic model (4.1) restricts all eigen-

modes to be antisymmetric. Therefore the model is of value only if only antisymmetric forcings are present. In particular, we have to expect the model to fail if strong disturbances of tropical heating, which are not symmetric to the equator, appear. To check this possibility we analysed the global distribution of 300 hPa velocity potential. Based on a global S-hierarchy, we found a significant and recurrent signal in this quantity (Fig. 12). The pattern is certainly not very symmetric.

- * The quasigeostrophic formulation of the model completely ignores the advection of eddy vorticity by the mean divergent wind field which has been shown to be of importance especially in the subtropics (Sardeshmukh and Hoskins, 1988; Held and Kang, 1987).

For the sake of completeness we have to mention that we performed a sensitivity analysis for the A-eigenmodes also. The statistical results are almost unaltered by moderate changes in the configuration of the basic flow $\bar{\Psi}$. The sensitivity to the diffusion constant ϵ is such that an increase by two orders of magnitude decreases the significance and the level of recurrence but hardly alters the reconstructed variance.

An interesting question is if our model results are in accord with the outcome of other GCM experiments on the effect of nontropical SST anomalies. We found a rising (lowering) of sea level pressure over and downstream the lowered (increased) SST. A similar behaviour was found by Chervin et al. (1980) who considered the effect of subtropical and midlatitude SST anomalies in the Pacific. Using different versions of the GISS model Hannoschöck and Frankignoul (1985) and Frankignoul and Molin (1988a,b) found conflicting responses to North Pacific SST anomalies, namely either a response similar to ours or a nonsignificant low level response. Palmer and Sun (1985) and Pitcher et al. (1988) simulated the effect of SST anomalies in the North Pacific and the North Atlantic and found a qualitatively different response, namely negative, largely equivalent barotropic height anomalies downstream of negative SST anomalies.



12. Significant and recurrent signal from a global S hierarchy of the 300 hPa velocity potential in the "cold vs. warm" experiment, units m^2/sec , contour interval $2.0 \cdot 10^5 \text{ m}^2/\text{sec}$.

6. The linearity of the response: Analysis of the "warm vs. control" and the "cold vs. control" experiments

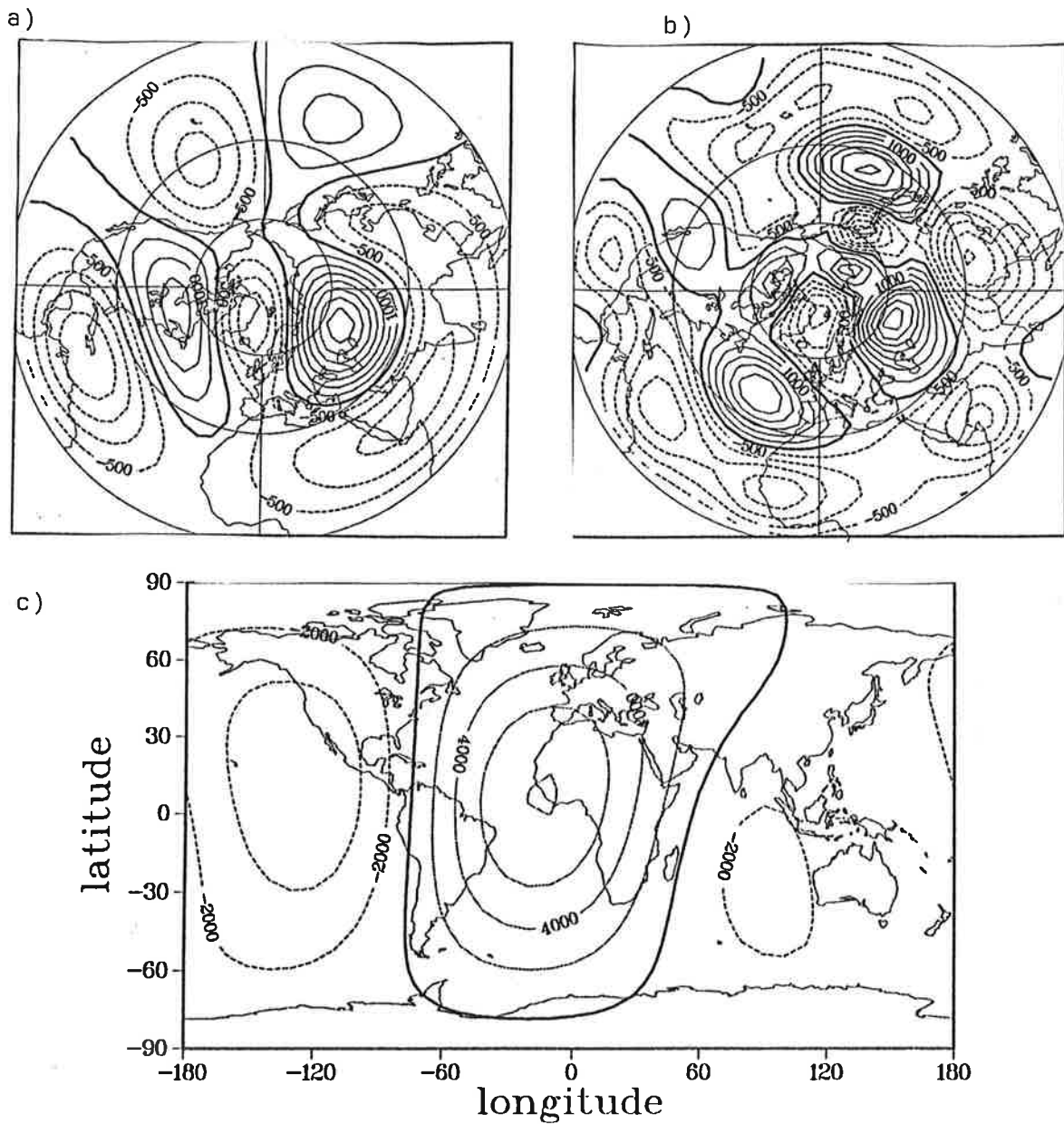
The third experiment "control" provides us with the possibility to study the T21 response with respect to the strength of the imposed boundary changes. With respect to "control" both anomaly experiments, "warm" and "cold", operate with the same SST anomaly pattern. The strength of the SST anomaly pattern in the "cold" ("warm") experiment is about 2/3 (1/3) of the "cold vs. warm" experiment. Therefore the "warm" experiment is considered as being a "small disturbance" experiment and the "cold" as a "medium disturbance" experiment.

6.1. LOW LEVEL TEMPERATURE

In the small amplitude disturbance experiment, "warm vs. control", no signal is identified in both the S- and the A-hierarchies. In the "medium disturbance" experiment a significant and recurrent signal appears in the A-hierarchy but not in S. The A-filtered response patterns of the "cold vs. control" and the "cold vs. warm" experiments are very similar (not shown). We conclude that the low level anomalous heating in our experiments is linear with respect to the imposed changes in SST and that the anomalous heating is balanced at low levels by anomalous advection.

6.2. 300 hPa STREAMFUNCTION

Testing the response of the 300 hPa streamfunction to the small SST anomaly (warm vs. control) yields a weak signal in the S-hierarchy (risk: 10%, level of recurrence: 80%) which explains 45% of the total variance. The B-hierarchy, however, leads to a considerable amplification of the signal, explaining more than 60% of the full signal, with a risk of 5% and a recurrence level of 90%. This result is insensitive to small variations in the basic flow. Both the B- and S-filtered pattern (Fig. 13) are broadly similar and differ markedly from the significant and recurrent pattern identified in the "cold vs. warm" experiment (Fig. 10), in particular over the Atlantic sector and over Asia. Concerning the tropical forcing mechanism we also found a (weak) signal in a global S hierarchy for "warm vs. control" in the 300 mb velocity potential. The reconstructed pattern (Fig. 13c) exhibits a monopole like structure with anomalous outflow over the tropical Atlantic. The pattern is almost symmetric to the equator thus allowing a mostly antisymmetric vorticity forcing.



13. Results from the "control vs. warm" experiment. (a) "Significant and recurrent" 300 hPa geostrophic streamfunction signal in the S-hierarchy, units m^2/sec , contour interval $5.0 \cdot 10^5 \text{ m}^2/\text{sec}$; (b) "significant and recurrent" 300 hPa geostrophic streamfunction signal in the B-hierarchy, contour interval as in (a); (c) "significant and recurrent" 300 hPa velocity potential signal in the S-hierarchy, units m^2/sec , contour interval $2.0 \cdot 10^5 \text{ m}^2/\text{sec}$.

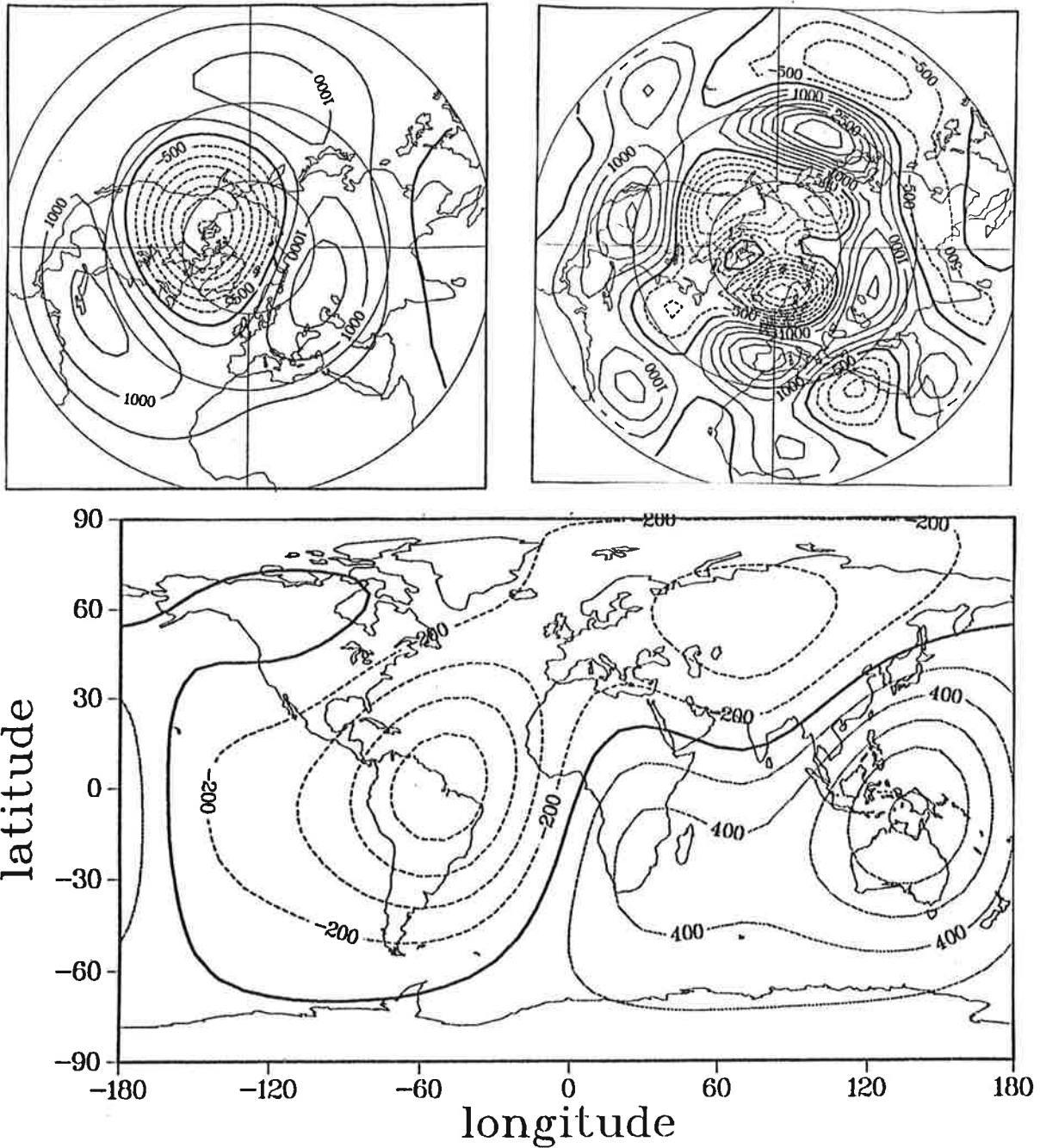
The "cold vs. control" signal appears weak in the S-hierarchy (risk: 10%, level of recurrence: 75%). A significant and recurrent signal is identified in the B-hierarchy (risk 5%, level of recurrence: 81%). In contrast to the previous results, however, the latter result shows some sensitivity to the choice of the basic flow. Although this may introduce some arbitrariness in the interpretation we present Fig. 14 for completeness. The B- as well as the S-filtered patterns exhibit some similarity with the "cold vs. warm" experiment. The tropical forcing, in terms of upper air velocity potential (Fig. 14c), deviates strongly from symmetry.

From the performance of the B-hierarchy in the three experiments, "cold vs. warm", "cold vs. control" and "warm vs. control", we conclude that the upper air streamfunction response may be well represented by the linear barotropic model only in the "warm vs. control" experiment, i.e. only the "warm vs. control" SST anomaly leads to a "small disturbance" which would allow for the linearization of the physics. This is in contrast to the results for the lower layers and supports our "two mechanisms" hypothesis.

7. Summary

We can make the following points regarding the modelled response to anomalous Atlantic SST:

- * The imposed changes in Atlantic SST lead to a change in surface pressure which is in broad agreement with the observations. Thus the observed decadal changes in SST are linked to atmospheric changes that were both observed and modelled. Certainly the GCM used is not capable to deliver a reliable regional climatic "forecast". But we are convinced that the model is able to describe an adequate first guess of the real changes.
- * The imposed midlatitude SST changes induce an anomalous surface heating which is balanced by horizontal linear advection of the mean flow at 1000 hPa thereby altering the low level temperature structure of the GCM ("mechanism 1"). The relationship between imposed SST changes and temperature appears to be linear as far as one can state this point from three samples. This result is in agreement with the theoretical works by Egger (1977) and Webster (1981), with the observational study by Barnett et al. (1984) and with many GCM experiments (Rowntree, 1979). It is, however, in conflict



14. Results from the "control vs. cold" experiment. (a) "Significant and recurrent" 300 hPa geostrophic streamfunction, signal in the S-hierarchy, units m^2/sec , contour interval $5.0 \cdot 10^5 \text{ m}^2/\text{sec}$; (b) "significant and recurrent" 300 hPa geostrophic streamfunction signal in the B-hierarchy, contour interval as in (a); (c) "significant and recurrent" 300 hPa velocity potential signal in the S-hierarchy, units m^2/sec , contour interval $2.0 \cdot 10^5 \text{ m}^2/\text{sec}$.

with the GCM studies by Palmer and Sun (1985) and Pitcher et al. (1988) who found their GCMs to generate penetrating responses to midlatitude SST anomalies.

- * The response of the upper tropospheric flow seems to result from changes in the convective activity which are due to the imposed SST variations and which in turn change the upper tropospheric divergence patterns. This acts as an anomalous vorticity forcing for the mean flow at 300 hPa. It initiates small, almost linear variations in the flow for the weak anomaly case "control vs. warm" but apparently a more complex relationship for the stronger anomaly cases "control vs. cold" and "cold vs. warm" ("mechanism 2").

ACKNOWLEDGEMENTS

We are indebted to Harry van Loon (NCAR) for suggesting the GCM experiments. Dr. O. Höflich gave valuable comments on the quality of the HSST data set, and Ingo Jessel and Heiko Borgert helped us with processing the data. Financial support was given by the "Klimaprogramm der Rheinisch-Westfälischen Akademie der Wissenschaften" under Prof.H. Flohn and from the Bundesministerium für Forschung und Technologie. Dr. Barbara Burns gave valuable advice on the English.

REFERENCES

- [1] Alexander, R.C. and R.L. Mobley, Monthly average sea-surface temperatures and ice - pack limits on a 1° global grid (1976) **Mon. Weath. Rev.**,104,143-148
- [2] Barnett, T.P., R.W. Preisendorfer, L.M. Goldstein and K. Hasselmann, Significance tests for regression model hierarchies (1981) **J. Phys. Oceanogr.**,11, 1150-1154
- [3] Barnett, T.P., H.D. Heinz and K. Hasselmann, Statistical prediction of seasonal air temperatures over Eurasia (1984) **Tellus**,36A, 132-146
- [4] Branstator G., Analysis of general circulation model sea - surface temperature anomaly simulations using a linear model. Part I: forced solutions (1985a) **J. Atmos. Sci.**,42, 2225-2241
- [5] Branstator G., Analysis of general circulation model sea - surface temperature anomaly simulations using a linear model. Part II: Eigenanalysis (1985b) **J. Atmos. Sci.**,42, 2242-2254
- [6] Chervin, R.M., J. E. Kutzbach, D.D. Houghton and R.G. Gallimore, Response of the NCAR general circulation model to prescribed changes in ocean surface temperature. Part II: Midlatitude and subtropical changes, (1989) **J.Atmos. Sci.**,37, 308-322
- [7] Dickson R.R., S.A. Malmberg, S.R. Jones and A.J. Lee, An investigation of the earlier great salinity anomaly of 1910-14 in waters west of the British Isles (1984) **ICES CM 1984/GEN 4**,15pp, cited after : Dickson, R.R., J. Meinke, S.A. Malmberg and A.J. Lee, The great salinity anomaly in the northern North Atlantic 1968-82 (1988) **Prog. in Oceanography**
- [8] Egger, J., On the linear theory of the atmospheric response to sea surface temperature anomalies (1977) **J.Atmos. Sci.**,34,603-614
- [9] Fischer G., Climate Simulations with the ECMWF T21-Model in Hamburg (1987) **Meteorologisches Institut Large Scale Atmospheric Modelling Report**,1,159pp

- [10] Frankignoul C. and A. Molin, Response of the GISS general circulation model to a midlatitude sea surface temperature anomaly in the North Pacific, (1988a) **J. Atmos. Sci.**,45,95-108
- [11] Frankignoul C. and A. Molin, Analysis of the GISS GCM response to a subtropical sea surface temperature anomaly using a linear model (1988b) **J. Atmos. Sci.**,45,3833-3845
- [12] Glowienka, R., Studies on the variability of Icelandic low and Azores high between 1881 and 1982, (1985) **Beitr. Phys. Atmosph.**,58,160-170
- [13] R. Glowienka-Hense, Statistische Analyse der Nordatlantik Oszillation im Bodendruck: Beobachtungen (1881-1984) and Simulation im Zirkulationsmodell T21, sowie die Rolle der Temperatur der Meeresoberfläche (1987) **Meteorologisches Institut der Universität Bonn**90pp
- [14] R. Glowienka-Hense, Performance of the ECMWF T21 model in simulating the North Atlantic Oscillation (NAO) (1988) **Climate Simulations with the ECMWF T21-model in Hamburg, Part II**, H.v.Storch (Ed.),35 - 51
- [15] G.Hannoschöck and C.Frankignoul, Multivariate statistical analysis of a sea surface temperature anomaly experiment with the GISS general circulation model, (1985) **J. Atmos. Sci.**,42,1430-1450
- [16] Hasselmann, K., On the signal - to - noise problem in atmospheric response studies (1979) **Meteorology over the tropical oceans**,251-259, Roy. Met. Soc., London
- [17] Held, I. and Kang, I.-S., Barotropic models of the extratropical response to El Niño (1987) **J. Atmos. Sci.**,44,1433-1452
- [18] A. Hense, Multivariate statistical analysis of the Northern Hemisphere circulation during the El Niño 1982/83 (1986) **Tellus**, 38A,189-204
- [19] Höflich W., The seasonal and secular variations of the meteorological parameters on both sides of the ITCZ in the Atlantic ocean, in (1974) **GARP Report**,2

- [20] Jones, P.D., S.C.B. Raper, B.S. Santer, B.S.G. Cherry, C. Goodess, R.S. Bradley, H.F. Diaz, P.M. Kelly and T.M.L. Wigley: A gridpoint surface air temperature data set for the Northern Hemisphere, 1851-1984. - DoE technical Report No. 22 (1985) **DoE Technical Report**,22, US Department of Energy Carbon Dioxide research Division, Washington DC, 251pp
- [21] Navarra A. and K. Miyakoda, Anomaly General Circulation Models, (1988) **J. Atmos. Sci**,45,1509-1530
- [22] Okamoto M., An asymptotic expansion for the distribution of the linear discriminant function (1963) **Annals of Math. Statist.**,34, 1286-1301
- [23] Page J.T., Error rate estimation in discriminant analysis (1985) **Technometrics**,27,189-198
- [24] Palmer, T..N. and Sun Zhaobao, A modelling and observational study of the relationship between sea surface temperature in the north-west Atlantic and the atmospheric general circulation, (1985) **Quart.J. Roy. Met. Soc.**,111,947-975
- [25] Pitcher, E.J., M.L. Blackmon, G.T. Bates and S. Munoz, The effect of North Pacific sea surface temperature anomalies on the January climate of a general circulation model, (1988) **J. Atmos. Sci.**,45,173-188
- [26] Rogers, J.C., Atmospheric circulation changes associated with the warming over the northern North Atlantic in the 1920s, (1985) **J. Climate Appl. Met.**,24,1303-1310
- [27] Rowntree, P.R., The effects of changes in ocean temperatures on the atmosphere (1979) **Dyn. Atmosph. Oceans**,3,373-390
- [28] Sardeshmukh P. and B.J. Hoskins, The generation of global rotational flow by steady idealized tropical divergence (1988) **J. Atmos. Sci.**,45, 1228-1252
- [29] Schneider, E.K., A formulation for diagnostic anomaly models, (1988) **PAGEOPH**,126,137-140

- [30] Simmon A.J., J.M. Wallace and G. Branstator, Barotropic wavepropagation and instability, and atmospheric teleconnection patterns, (1983) **J. Atmos. Sci.**,40,1363-1392
- [31] Storch, H. von, A statistical comparison with observations of control and El Niño simulations using the NCAR CCM (1987) **Beitr. Phys. Atmosph.**,60,464-477
- [32] Storch, H. von and F. Zwiers, Recurrence analysis of Climate sensitivity experiments, (1988) **J. Climat.**,1,157-171
- [33] Storch, H.von, Climate Simulations with the ECMWF T21-Model in Hamburg Part II: Climatology and sensitivity experiments (1988) **Meteorologisches Institut Large Scale Atmospheric Modelling Report**,4, 265pp
- [34] van Loon, H. and J. Rogers, The seesaw in winter temperature between Greenland and northern Europe. Part I: General description, (1978) **Mon. Wea. Rev.**,106,296-310
- [35] van Loon, H. and R.A. Madden, Interannual variations of monthly mean sea-level pressure in January, (1983) **J. Climate Appl. Met.**,22,687-692
- [36] Webster, P.J., Mechanism determining the atmospheric response to sea surface temperature anomalies (1981) **J. Atmos. Sci.**,38,554-571
- [37] Zwiers F. and H. von Storch, Multivariate Recurrence Analysis (1989) **J. Climat.**,2 in press; also: Max Planck Institut für Meteorologie Report 17 (1988)

FIGURE CAPTIONS

1. The first two January EOFs of the Historical Sea Surface temperature (HSST: [19] Höflich, 1972). After Glowienka-Hense (1987). (a) EOF1 (16%); (b) EOF2 (9%); pattern of EOF's are normalized to have an absolute maximum value of 10, contour lines are drawn in subjectively for better visualization (c) time amplitude of EOF1; (d) time amplitude of EOF2.
2. Observed air temperature anomaly in January at Funchal (Madeira). After the World Meteorological Station Climatology. According to Jones et al (1985) the time series does not suffer from inhomogeneities. Dashed: raw data; continuous line: 10 year running mean. Units: °C.
3. Significant and recurrent signal in the difference between the observed air pressure decadal means 1904-13 and 1951-60. Units: hPa, contour interval 1 hPa. Negative anomalies are dashed. (After Glowienka-Hense, 1987).
4. Decadal difference field of the Atlantic Ocean SST in January between 1904-1913 ("cold" experiment) and 1951-60 ("warm" experiment). The field is reconstructed from the first two January EOFs shown in Fig. 1. Units 10^{-2} °C, contour interval 0.25°C .
5. On the concept of recurrence. (a) Minimum difference of means, in units of standard deviations, which is identified by a t-test with probability of at least 90%, if the sample size of both ensembles increases (horizontal axis). (b) Schematic diagrams to illustrate the subdivision of the d -dimensional space into two complementary sets, S_i and S_j with $S_i \cup S_j = R^d$. Left: $d = 1$, the curves show the probability densities. The $d - 1 = 0$ dimensional hyperplane \mathcal{H} is a point on the horizontal axis. Right: $d = 2$, contour plot of the probability densities. The 1-dimensional hyperplane \mathcal{H} is the straight line. (After Storch and Zwiers (1988) and Zwiers and Storch (1988).)
6. Long term average geostrophic streamfunction in the warm and the cold experiment. (a) 300 hPa: the mean flow to derive the barotropic normal

modes of the B hierarchy, units m^2/sec , contour interval $10^7 \text{ m}^2/\text{sec}$, (b) 1000 hPa: the mean flow to derive the temperature advection normal modes of the A hierarchy, units m^2/sec , contour interval $5.0 \cdot 10^6 \text{ m}^2/\text{sec}$

7. Test statistic T^2 (top) and estimate of recurrence (bottom) as a function of A-hierarchy parameters for the 850/1000 hPa layer temperature in the "cold vs. warm" experiment. The continuous lines in the top panel are the indicated error levels for T^2 if the null hypothesis holds. The arrow marks the model which was selected as being "significant and recurrent".
8. 850/1000 hPa layer temperature signal in the "cold vs. warm" experiment. (a) total difference field, units m^2/sec , contour interval $10^5 \text{ m}^2/\text{sec}$; (b) level of local recurrence p , $p = 77$ (84)% corresponds to $q = 93$ (98)% in Storch and Zwiers (1988) and Eq. (3.5), units %, contour interval 5%; (c) "Significant and recurrent" signal in the S-hierarchy, contour interval as in (a); (d) "Significant and recurrent" signal in the A-hierarchy, contour interval as in (a).
9. 1000 hPa streamfunction signal in the "cold vs. warm" experiment. (a) total difference field, units m^2/sec , contour interval $5.0 \cdot 10^5 \text{ m}^2/\text{sec}$; (b) level of local recurrence p , $p = 77$ (85)% corresponds to $q = 93$ (98)% in Storch and Zwiers (1988) and Eq.(3.5), units %, contour interval 5%; (c) "Signifucant and recurrent" signal in the S-hierarchy, contour interval as in (a).
10. 300 hPa streamfunction signal in the "cold vs. warm" experiment. (a) total difference field, units m^2/sec , contour interval $5.0 \cdot 10^5 \text{ m}^2/\text{sec}$; (b) level of local recurrence p , $p = 77$ (85)% corresponds to $q = 93$ (95)% in Storch and Zwiers (1988) and Eq.(3.5), units %, contour interval 5%; (c) "Significant and recurrent" signal in the S-hierarchy, contour interval as in (a).
11. Meridional average, as a function of longitude and height, of the S-filtered streamfunction anomalies in the "cold vs. warm" experiment. units m^2/sec , contour interval $5.0 \cdot 10^5 \text{ m}^2/\text{sec}$; (a) $0^\circ\text{N} - 30^\circ\text{N}$; (b) $30^\circ\text{N} - 60^\circ\text{N}$; (c) $60^\circ\text{N} - 90^\circ\text{N}$.

12. Significant and recurrent signal from a global S hierarchy of the 300 hPa velocity potential in the "cold vs. warm" experiment, units m^2/sec , contour interval $2.0 \cdot 10^5 \text{ m}^2/\text{sec}$.
13. Results from the "control vs. warm" experiment. (a) "Significant and recurrent" 300 hPa geostrophic streamfunction signal in the S-hierarchy, units m^2/sec , contour interval $5.0 \cdot 10^5 \text{ m}^2/\text{sec}$; (b) "significant and recurrent" 300 hPa geostrophic streamfunction signal in the B-hierarchy, contour interval as in (a); (c) "significant and recurrent" 300 hPa velocity potential signal in the S-hierarchy, units m^2/sec , contour interval $2.0 \cdot 10^5 \text{ m}^2/\text{sec}$.
14. Results from the "control vs. cold" experiment. (a) "Significant and recurrent" 300 hPa geostrophic streamfunction, signal in the S-hierarchy, units m^2/sec , contour interval $5.0 \cdot 10^5 \text{ m}^2/\text{sec}$; (b) "significant and recurrent" 300 hPa geostrophic streamfunction signal in the B-hierarchy, contour interval as in (a); (c) "significant and recurrent" 300 hPa velocity potential signal in the S-hierarchy, units m^2/sec , contour interval $2.0 \cdot 10^5 \text{ m}^2/\text{sec}$.